Long-term creep and shrinkage in concrete using porous aggregate – the effects of elastic modulus

Jón Guðni Guðmundsson

Thesis of 90 ECTS credits
Master of Science in Civil Engineering with Specialization in Concrete Technology
January 2013

Long-term creep and shrinkage in concrete using porous aggregate – the effects of elastic modulus

Jón Guðni Guðmundsson

Thesis of 90 ECTS credits submitted to the School of Science and Engineering
at Reykjavík University in partial fulfillment
of the requirements for the degree of
**Master of Science in Civil Engineering with
Specialization in Concrete Technology**

January 2013

Supervisor:

Dr. Ólafur H. Wallevik
Professor, Reykjavik University, Iceland
Professor (adjunct), Université de Sherbrooke, Canada

Examiner:

Dr. Kamal Khayat
Professor, Missouri university of Science and technology
Professor, Université de Sherbrooke, Canada
Professor (Associate), Reykjavik University, IcelandTough E. Questions,

Long-term creep and shrinkage in concrete using porous aggregate – the effects of elastic modulus
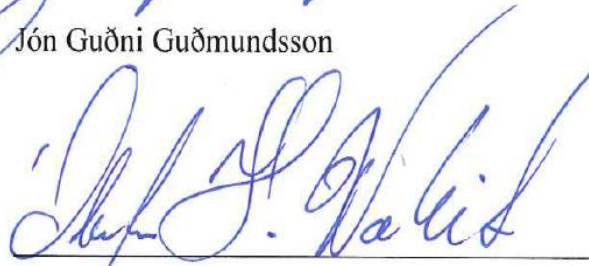
Jón Guðni Guðmundsson

90 ECTS thesis submitted to the School of Science and Engineering
at Reykjavík University in partial fulfillment
of the requirements for the degree of
**Master of Science in Civil Engineering with
Specialization in Concrete Technology**

January 2013

Student:

Jón Guðni Guðmundsson

Supervisor:

Dr. Ólafur H. Wallevik

Examiner:

Dr. Kamal Khayat

Abstract

Long-term deformation is a problem of concrete structural elements when using porous basaltic aggregate, indicating concrete beams and plates subjected to sustained loading. Icelandic basalt is typically very porous and is often quite amorphous, which significantly affects the modulus of elasticity of the concrete and the dependent restraint to creep deformation of the aggregate. Research on the long-term creep of concrete made with porous basaltic aggregate was undertaken at the ICI Rheocenter where data collected over 10 years were being used for analysis. The available data shows that there is greater creep in Icelandic concrete compared to e.g. concrete with Norwegian aggregates. Creep data was compared to three well accepted models, EuroCode 2 model, ACI209 model and the B3 model by Bazant [1]. Findings indicate that concrete with porous basaltic aggregate exhibits greater creep than predicted values and the difference is in some cases over 40% higher.

Research on the effects of aggregate type and porosity on the elastic behavior of the concrete composite was conducted. The focus was to get confirmed the relations between the elastic modulus of the concrete and the increased porosity of the aggregate. The main scope was to establish connection between increased porosity of aggregate on concrete creep and shrinkage. The creep of concrete is interlinked to the elastic modulus of the concrete and if the increased porosity of the aggregate reduces the elastic modulus, the creep of the concrete is obviously affected.

Research on the effects the porosity of the aggregate on the mechanical properties gave a significant indication of correlation between increased porosity and decrease in mechanical properties. The elastic modulus of the aggregate was shown to be inconclusively in connection to the porosity of the material, where increased porosity from 3% to 6% lowers the elastic modulus by about 7GPa. There is a strong correlation of the density of the aggregate to the elastic modulus of the aggregate. The final conclusion was that concrete composite is affected by increased porosity of aggregate. This gave the connection that if the porosity of the aggregate reduces the elastic modulus of the concrete the volume stability is compromised and the concrete creeps and shrinkage is greater.

Ágrip

Langtíma niðurbeygja er vandamál í steyptum einingum þegar notast er við basalt með háa holrýmd, samanber plötur og bita undir jöfnu langtímaálagi. Íslenskt basalt er yfirleitt með háa holrýmd og inniheldur oft mikið af gleri. Rannsóknir á langtímaskriði á steypu þar sem notast er við fylliefni með háa holrýmd hafa verið framkvæmdar og gögnum safnað í meira en 10 ár hjá Nýsköpunarmiðstöð Íslands. Fyrirliggjandi gögn sýna að það er meira skrið í íslenskri streypu en steypu þar sem notast er við t.d. norsk fylliefni. Skrið var borið saman við þrjú vel viðurkennd líkön, EuroCode 2 líkan, líkan frá American Concrete Institute og líkan sem hannað er af Bazant og kallast B3. Niðurstöður voru að steypa þar sem notast er við fylliefni með háa holrýmd skríði töluvert meira en líkönin áætla og í sumum tilfellum yfir 40% meira.

Áhrif ólíkra tegunda fyllefna með mismunandi holrýmd á fjaður eiginleika steypu voru einnig til athugunar. Áhersla var lögð á að skoða tengsl fjaðurstuðuls steypu við aukna holrýmd fylliefna. Meiginmarkmiðið var á að sýna fram á tengsl aukinnar holrýmdar fylliefna við skrið og rýrnun steinsteypu. Skrið steinsteypu er háð fjaðurstuðli steypu og ef holrýmd fylliefna eykst lækkar fjaðurstuðull steypunnar, sem hefur þar af leiðandi áhrif á skrið hennar.

Niðurstöður rannsóknir á áhrifum hárrar holrýmdar á burðarþolseiginleika fylliefna gáfu til kynna skýrt sambnad milli holrýmdar og lækkunar burðarþolseiginleika. Sýnt er fram á að tengsl eru á milli fjaðurstuðull fylliefnanna og holrýmd efnisins, þar sem holrýmdaraukning úr 3% í 6% lækkar fjaðurstulinn um 7 GPa. Sterk tengsl voru á milli þéttleika efnisins og fjaðurstuðuls. Endanleg niðurstaða er því sú að holrýmd fylliefna hefur veruleg áhrif á steinsteypu. Holrýmd fylliefnanna lækkar fjaðurstuðul steypu, rúmfræðilegur óstöðugleiki eykst og steypan fer að skríða og rýrna meira.

Acknowledgments

Table of Content

Table of Figures

List of Tables

Notions and Symbols

Abbreviations:

ACI	–	American Concrete Institute
C-S-H	–	Calcium silicate hydrate
CO_2	–	Carbon dioxide
CVC	–	Conventional vibrated concrete
EC2	–	EuroCode 2
GPa	–	Giga-Pascal
HPC	–	High performance concrete
HSC	–	High strength concrete
ITZ	–	Interfacial transition zone
MPa	–	Mega-Pascal
OPC	–	Ordinary Portland cement
RH	–	Relative ambient humidity
SCC	–	self compacting concrete

Symbols:

α	–	Degree of hydration
A	–	Area
A_c	–	Area of a concrete section
A^c	–	Free energy for cracking
β	–	Factor for describing stage 2 of the creep law
β_c	–	Time coefficient for creep calculations in EC2
β_H	–	Factor for environmental condition in EC2
β_{ds}	–	Time coefficient for dry shrinkage calculations in EC2
β_{as}	–	Time coefficient for autogenous shrinkage calculations in EC2
c	–	Creep deformation
C	–	Elasticity tensor
δ	–	Deformation
D	–	Effective thickness
ε	–	Strain
$\boldsymbol{\varepsilon}$	–	Strain tensor
ε_0	–	Initial strain
ε_t	–	Final strain
ε_c	–	Creep strain
ε_{cc}	–	Total creep strain according to EC2 at time t
ε_{cs}	–	Total shrinkage strain according to EC2
ε_{cd}	–	Drying shrinkage strain according to EC2
ε_{ca}	–	Autogenous shrinkage strain according to EC2

ε_h	–	Hygrothermal
ε_v	–	Viscoelastic strain
ε_f	–	Viscous strain
ε_{volume}	–	volumetric strain
$(\varepsilon_{sh})_u$	–	ultimate shrinkage strain
E	–	Elastic modulus
E_c	–	Elastic modulus of concrete
E_m	–	Elastic modulus of mortar
E_A	–	Elastic modulus of aggregate
E_{cp}	–	Elastic modulus of cement paste
φ	–	Creep coefficient
f_c	–	Strength of concrete
f_{ck}	–	Characteristic strength of concrete
f_c'	–	Specific strength of concrete
γ	–	Shear strain
γ_c'	–	Unit weight of concrete
γ_c	–	Creep coefficient for creep in ACI209
γ_{sh}	–	Shrinkage coefficient for creep in ACI209
G	–	Shear modulus
G'	–	Gibson energy
h_0	–	Notional size defined in EC2
I	–	Second moment of inertia
$J(t,t_0)$	–	Compliance function for creep deformation
κ	–	Factor describing stage 3 of the creep law
K	–	Bulk modulus
L	–	Length
M	–	Momentum
ρ_c	–	Density of cement
ρ_w	–	Density of water
ρ_{SSD}	–	Density of aggregate under surface saturated dry conditions
P	–	Force
p_t	–	Porosity of cement paste
r	–	Radius of curvature
σ	–	Stress
$\boldsymbol{\sigma}$	–	Stress tensor
σ_c	–	Concrete stress
σ_l	–	Lateral stress
σ_0	–	Initial stress
σ_{volume}	–	volumetric stress
S_h	–	Shrinkage deformation

S_T	–	Temperature deformation
τ	–	Shear stress
τ_{av}	–	Average shear stress
t	–	Time/age
t_0	–	Age at loading
$t´$	–	Age when exposed to drying
ΔT	–	Temperature difference
u	–	Parameter to define part of a cross section exposed to drying
υ	–	Poisson´s ratio
v_u	–	Ultimate creep strain
V	–	Volume
V_s	–	Volume of solid materials
V_v	–	Void volume
V_w	–	Volume of water
V_a	–	Volume of air
V_A	–	Volume of aggregate
V_{CP}	–	Volume of cement paste
ω_{sat}	–	Water absorption
W	–	Shear force
W_s	–	Weight of solid materials
W_w	–	Weight of water
W_t	–	Total weight
w/c	–	Water to cement ratio

1. Introduction

A lot of data on shrinkage and creep in Icelandic concrete has been collected through the years at the ICI Rheocenter, this data shows that there is considerable more creep and shrinkage in Icelandic concrete. The shrinkage is about 1 mm/m and is considered to be caused by other factors than the cement. The results have shown that Icelandic concrete has a tendency to shrink more than concrete from other countries and this is in line with the theory that the more porous the aggregate are the more shrinkage the concrete experiences. Studies have been done on many types of concrete and all of them have shown this tendency. The creep of concrete using Icelandic porous basalt aggregate is significantly higher in most cases compared to concrete using granite with low porosity. The results highly suggest that the porous aggregate used in Iceland is increasing the creep due to the increased porosity. This mater has to be studied and this is the subject of the research presented in the thesis.

Long term deformation has been a problem of concrete structure elements in Iceland, e.g. in concrete beams and plates. This long term deformation is caused by long term creep which is a great deal more in concrete containing Icelandic aggregates (basalt) than in concrete made from other aggregates (foreign aggregates). Long term creep can also have a very negative effect on the performance of prestressed concrete elements. The main factors that have the most effect on concrete creep (with the exception of load) and shrinkage are type of aggregate, cement type and water-cement ratio (w/c ratio). In Iceland all these factors are different to what is considered normal practice. Cement in Iceland is made from shell debris and rhyolite instead of limestone and clay. Due to this, the volume of cement paste constitutes a greater part of the concrete volume in Iceland than in e.g. Scandinavia. The main benefits of this research study are in the field of concrete technology and the design of concrete structures. The aim of the research study is to establish the influence of porosity of the aggregates on creep and shrinkage. The outcome of the thesis is also meant to assist in model building for describing deformation in concrete containing porous aggregates.

The work is divided into two phases, research on long-term creep and shrinkage of concrete and the elastic modulus of concrete composite and porous aggregate. In the first phase there will be conducted a thorough study on the research conducted on creep and shrinkage for over a decade. Using the research data to compare to design standards and theories on why the concrete using Icelandic porous basalt seems to creep more than predicted data. In the first phase of the work there will be a comparison of concrete made with Icelandic porous aggregate against the data for concrete made with Norwegian dense granite aggregate. All the data will be presented and analyzed in such away so it can be contemplated how to prepare better for the increased concrete creep and shrinkage.

In second phase of the work, research on aggregate properties will be conducted; with a main focus on the porosity of the material and how that affects the mechanical behavior of the aggregate. The main research will be carried out on aggregate cores taken from two quarries in Iceland. Theses cores will be tested for porosity using two methods to evaluate the testing methods used. The mechanical properties will then be measured using commonly used methods

(standardized methods) and those properties compared to the porosity of the aggregate cores. This will give a good idea on how much the properties are affected by the porosity. This will then be used to model the elastic modulus of the concrete using simple models to see just how much the porosity of the aggregate effects the concrete composite.

2. Fundamentals of structural concrete

In this chapter there will be a discussion on the fundamental aspects of structural behavior concerning concrete structures. In that retrospect the stress and strain of structural elements will be defined and other common structural behavior. There will be a brief discussion on what concrete is made of and how it's made. The creep and shrinkage behavior of solids will be discussed. Concrete creep will be discussed in detail and theories on the mechanism of concrete creep presented. Basic creep and drying creep will be defined and the difference between them discussed. As shrinkage is an interconnected part of concrete creep it will be classified and gone over in detail. Aggregates are a fundamental part of the concrete as it takes more than half the volume of a concrete body. There for, aggregates and there affects on concrete and especially concrete creep will be discussed.

2.1   Structural basics

The distribution of stresses in cross section of a structural member is categorized in two types although there are four types of internal forces. There is one that acts perpendicular to the cross section and one which acts tangentially to the cross section, i.e. direct stress and shear stress. This distribution of these stresses is dependent on the internal force system of the structural member and the geometry of the cross section. In some cases these distributions are complex, e.g. in the case of bending or shearing in an unsymmetrical cross section .

Direct stress is defined as the stress perpendicular to the cross section of a structural member and the simplest form for this stress is produced by an axial load. By taking a cross section that has an area of A with an axial force P that acts perpendicular to it. An illustration of this Then the direct stress is defined as follows:

$$\sigma = \frac{P}{A} \tag{1}$$

Here it is assumed that the force P is uniformly distributed over all the area of the section A. The direct stress can both be in compression and tension and is measured in Pa (N/m^2) in SI units.

Shear stress is defined as the stress that acts tangentially to the cross section of a structural member and is produced by a shear load. The cross section has the area of A and there is as shear force W acting tangentially on the cross section. The average shear stress τ_{av} is defined as the force divided by area as it is assumed to be uniformly distributed. This is shown in Figure 1 and is formulated as follows:

$$\tau_{av} = \frac{W}{A} \tag{2}$$
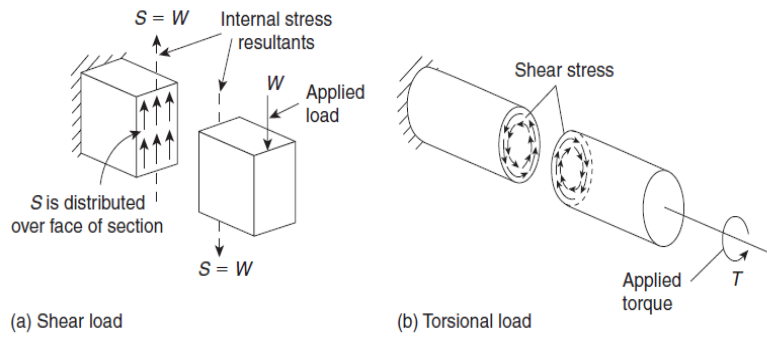
Figure 1: (a) Shear stress in an element from vertical loading, (b) Shear stress in an element were torque is applied

Shear stress can also occur in a circular section where there is applied torque. There the shear stress is tangentially to the plan of rotation.

As load is applied to a member it disorder as no material is completely ridged. The deformation increases in tension and decreases in compression. The deformation δ of a member of length L when load is acting on it, strain is defined as the deformation divided be the length of the member. This is formulated as:

$$\varepsilon = \frac{\delta}{L} \tag{3}$$

Strain is defined as dimension less but sometimes represented in ‰ or ppm (part per million). There are also other types such as shear strain which is induced by shear stress. The shear strain can be defined as the change in the angle γ between two originally mutually perpendicular edges, this is illustrated in Figure 2. This strain is measured in radians. Another type of strain is hydrostatic strain which acquire, when an element is affected by hydrostatic pressure. This means the element is under uniform stress at all sides, e.g. for a cube this mean equal stress at all six sides of the cube (shown in Figure 3) [2].

19
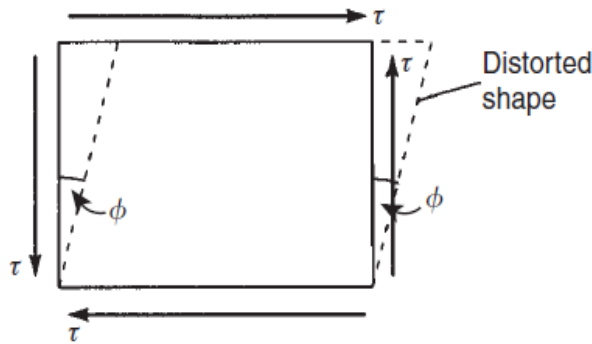
Figure 2: Shear strain defined as an angle between perpendicular edges
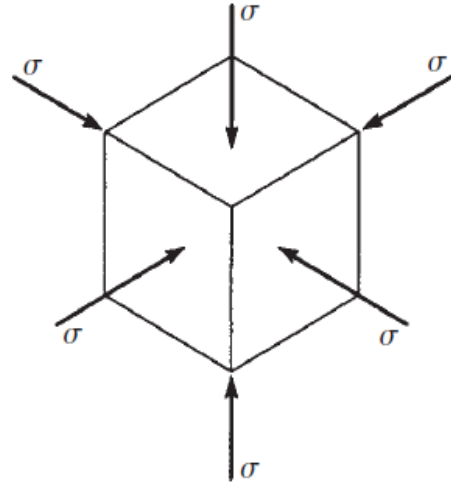
Figure 3: Hydrostatic strain uniformly distributed over the hole element, as is the hydrostatic pressure

Stress-Strain relationship

To measure stress strain relationship a tensile test is used. In the test a known axial tensile load is applied to the specimen at specified increments and measuring the corresponding length changes. Then a curve like in Figure 4 is acquired which represents the stress-strain relations. The linear relationship (line a-b) between stress and strain in the beginning of the curve is called Hooke´s law. Robert Hooke discovered it first in year 1678 and it can be mathematically described by the following formula:

$$\sigma = E\varepsilon \tag{4}$$

Here the constant E is the elastic modulus or Young´s modulus. It has the same units as stress i.e. MPa and e.g. steel has an elastic modulus of 200.000 MPa (200 GPa). For a lot of materials the modulus is the same in tension and compression [2].
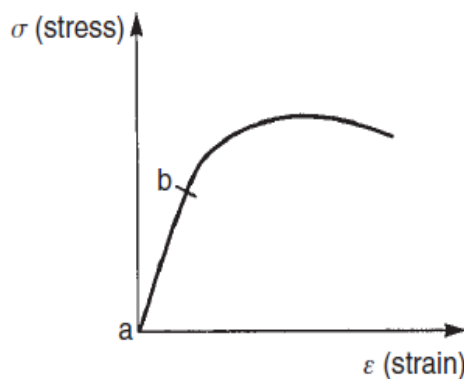
Figure 4: Typical stress-strain curve for concrete

Same as for direct stress and strain, the relationship between shear stress and shear strain is formulated using a linear relationship. It is formulated as follows with a constant G called the shear modulus:

$$\tau = G\gamma \tag{5}$$

There is also another relationship called the volume modulus or bulk modulus and is defined as the volumetric stress divided by the volumetric strain [2]. It is formulated as follows:

$$K = \frac{\sigma_{volume}}{\varepsilon_{volume}} \tag{6}$$

It is a common experience that when you stretch an elastic material the cross section becomes smaller. This behavior of the material is defined as the Poisson effect and is also observed in structural material under both tension and compression. In the elastic region of stress-strain relationship (i.e. where the curve is linear) there is constant relationship between lateral and longitudinal strain which is called the Poisson's ratio and the symbol v is normally used for it. There is a schemaic picture of this behavior in Figure 5. The material constants *E, G, K* and v are known as the elastic constants.By using the Poisson ratio it is possible to interlink the elastic constants E, G, K. They are interlinked as follows [2]:

$$E = 2G(1 + v) \tag{7}$$

$$G = \frac{E}{2(1 + v)} \tag{8}$$

$$K = \frac{E}{3(1 - 2v)} \tag{9}$$
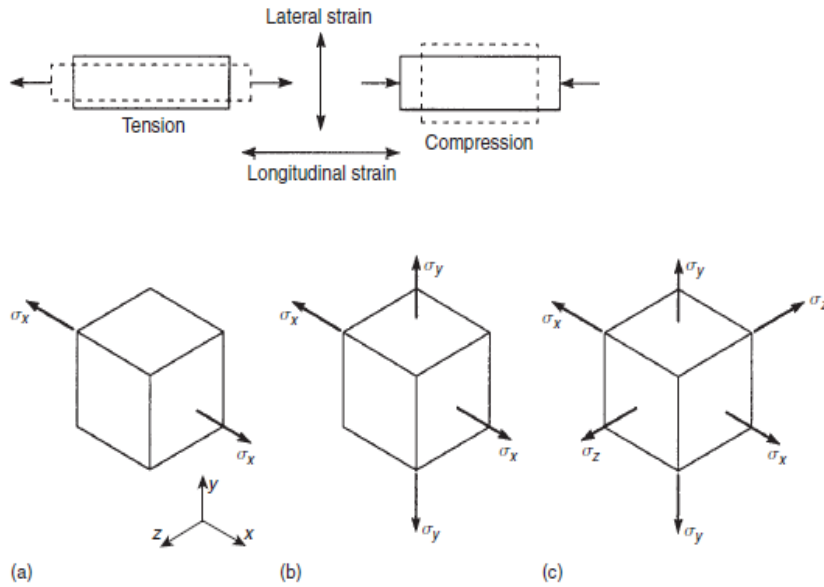
Figure 5: Poisson´s ratio between longitudinal and transversal directions of an element

Concrete Beams

Beams are linear structural elements that are mostly loaded generally in flexure and their response is generally governed by their flexural behavior and shear deformation can in most cases be ignored. So in this chapter a short introduction into the flexural behavior of beams will be presented. Based on the Hooke´s law the following can be assumed as the equation that describes the flexural behavior:

$$M = \frac{EI}{r} \tag{10}$$

Here M is the moment in the beam section, E is the elastic modulus of the material, I is the second moment of inertia of the section and r is the radius of curvature. Beams are most often analyzed assuming that the flexural rigidity is constant along the beam and many design aids are based on this conception. This is not completely true, especially for concrete beams. This is due to the fact that in bending the bottom of the concrete beam is subjected to tension and the beam cracks.

2.2   Structural Concrete

Concrete is made from two main components, stone (which are called aggregates) and the cement matrix which coats and links the aggregates. Aggregates are classified into two categories; fine aggregates which consist of sand with particle size 4 mm or lower (that is in Europe, in America it is 5 mm) and coarse aggregate which can be gravel or crushed aggregates [3].

Concrete is one of the main building material that humans uses to create there infrastructure and buildrings that are used every day. Concrete is a material that has been used for thousands of years, e.g. the Pantheon in Rome is constructed from concrete. Roman concrete was created in a similar mater as modern concrete, i.e. with similar ratios and materials [4]. Though it had lesser strength then modern concrete (about 20 MPa compared to a common strength classes having 25-30 MPa nowadays,[5]) the Romans could build marvels like the dome of the Pantheon. It is still has the world recorded for the larges span of a dome for a non-reinforced concrete building [6].

Modern concrete can be very various in its composition, it depends on what is what properties are needed in the construction or application. The concrete is though in nearly all cases made with OPC. There are many types of concrete, such as Self-consolidating concrete (SCC), High performance concrete (HPC) and High strength concrete (HSC, which is a type of HPC). These types can also have sub-classes such as semi-SCC (which is somewhere in between SCC and conventional vibrated concrete (CVC) in flow ability) and High durability concrete which is a type of HPC. Concrete is used in all sorts of infrastructure and buildings in modern society, from building such as underwater structures to highest skyscrapers, and from the longest bridges to the largest oilrigs. So in fact concrete is one of the greatest construction material ever invented because without it most of the marvels created by human kind in the modern world would never have been possible.

Composition of concrete

The main component of concrete is the cement which with water makes up the glue that makes up the matrix which in fact holds the aggregates together. The most common cement is ordinary Portland cement (OPC) and makes up most of the hydraulic binder (the glue) but in some cases, and in increasing manner, mineral admixtures are added such as fly ash, blast furnish slag and silica fume. These are all pozzolans [7, 8] and have latent hydraulic affects and are often well grounded. They are often used to replace cement for environmental purpose, because cement production creates allot of CO_2 emissions [9]. These mineral admixtures are also often used because they can change the properties of concrete, e.g. silica fume decreases the plastic viscosity of fresh concrete [10, 11]

Water is one of the main components in concrete because of the hydraulic process of the cement and water. Water also fills the void in the concrete and in fact as water becomes a greater part of concrete the voids increase in size. This is due to the fact that more water increases the length between particles before hydration and as hydration occurs, the voids in the system become greater as the distance between particles is large. This in fact decreases the strength of the concrete as voids are not supportive in the concrete structure.

A large proportion of the concrete are aggregate and in fact they are about 60%-80% of the volume of concrete. Aggregate come in many different sizes and shape and are defined into two main types, i.e. fine aggregate and coarse aggregate. As aggregate are such a large part of the concrete mix they affect the concrete allot and have a large effect on mechanical properties and rheology of fresh concrete [10]. Their main role in the concrete is to fill up the space in between the cement past to create the

unhydrated cement particles

cement gel

capiliary pores and cavities

A) Immediately after mixing
B) Reaction around particles – early stiffening
C) Formation of skeletal structure – first hardening
D) Gel infilling – later hardening

Figure 6: The hydration of cement particles [12]

strong cement matrix. They are also in most cases the cheapest part of the concrete mixture and the more volume they occupy the cheaper the concrete gets.

In modern structural concrete there is nearly always internal reinforcement and is an intricate part of the concrete structure. The main role of reinforcement is to take up tension loads in a concrete structure. As concrete has little tension strength but large compressive strength the reinforcement is a good way of completing the structural material as one of the greatest and most used building material around. Reinforcement is most often made of steel, but in recent years fiber reinforced bars have been used increasingly, i.e. fiber strings woven into bars and glued togather by epoxy. These new materials are considered a better chose where there is a threat of

corrosion as that is one of the main problem with using steel as reinforcement. Also the fibers can be used as just fibers in the concrete, e.g. to resist surface cracking due to plastic shrinkage.

2.2.1. Mechanical properties of concrete

Strength of concrete is the main mechanical property that engineers have defined concrete from, e.g. standards (such as EusoCode2 (EC2)) often give other properties as a function of compressive strength. One of the main properties of concrete is the elastic modulus and as concrete is a composite material the elastic behavior is governed by mainly two phases, the cement paste phase and the aggregate

Figure 7: Stress-strain relationship of concrete, shown together with the aggregate and cement paste

phase. The stress-strain relationship of both phases and the concrete are shown in Figure 7.

Concrete is a composite material as has been discussed, this makes the material constants differ by changing the composition. Most standards recommend the use of the compressive strength to evaluate the material constants. The concrete is often described as three phases; the cement paste, the aggregate and the connection between them called the interfacial transition zone (ITZ). In this section there will be a discussion on the elastic modulus of these phases of the concrete composite.

Cement past

Cement paste is basically the glue of the concrete that brings everything together. It is made from mostly cement and other cementitious materials such as silica fume and fly ash. The fines from the fine aggregate are also a part of the cement paste. The hydraulic products of the cement have been studied to determine the elastic modulus of the past. The findings have shown that the paste can have an elastic modulus ranging from 4 GPa to 25 GPa[2]. The elastic modulus depends largely on the capillary porosity of the cement paste. The porosity depends on the water-binder ratio; as the more water is in the system the longer distance is between cement particles.

The porosity of a normal mixture of concrete with w/c ratio between 0,25-0,60 can have about 0,25-0,50 in porosity[3]. This gives about 6-15 GPa in elastic modulus of the cement paste. The cement can have difference in elastic properties, depending on how the packing is subjected to the specimen. There are two phases of C-S-H gel that give two different values for elastic modulus, the C-S-H can have a value of 23,8 GPa. For a cement past with a 0,5 w/c ratio, the value is 15 GPa [4].

There are methods to calculate the capillary porosity of a concrete mixture from the w/c-ratio, degree of hydration and the density of the cement and is given by the following equation:

$$p_t = \frac{\frac{w}{c} - 0{,}17\alpha}{\frac{1}{\rho_c} + \frac{w}{c}} \qquad (11)$$

Where *w/c* is the water cement ratio, α is the degree of hydration and ρ_c the density of the cement. This behavior can be observed in Figure 8 as well as the decrease in elastic modulus of the mortar purposed by Zohdi [13].
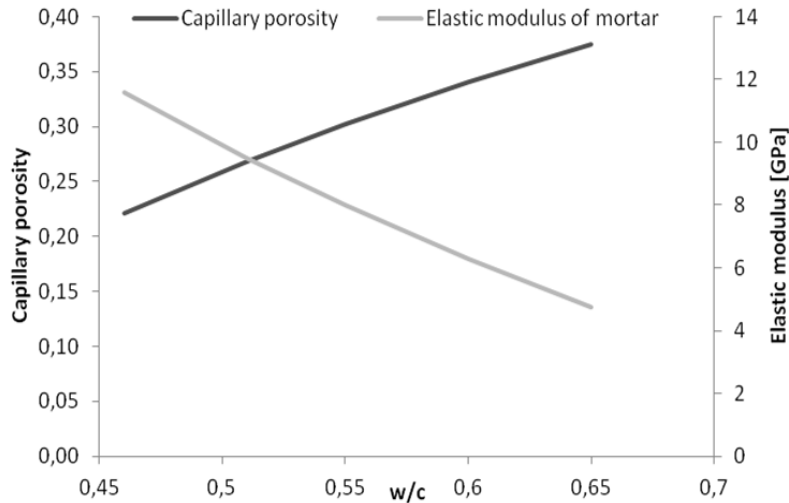
Figure 8: Capillary porosity and elastic modulus of cement paste as a function of w/c ratio

Concrete aggregate

Aggregate are one of the main components in concrete and make up about 60-75% of the volume of the composition. As aggregate are in most cases more stiff then cement paste, it is the main contributor the elastic modulus of the concrete. Aggregate can have very variant elastic depending on type and porosity of the material. For example basalt aggregate with low porosity can have a elastic modulus of 90 GPa, but the same material with high porosity can have upto 40 GPa [3, 15, 16].

Interfacial Transition Zone (ITZ)

The ITZ is the weakest phase of three composites, i.e. the cement paste, aggregate and the ITZ. IT is the zone between the cement paste and the aggregate which is about 0,02-0,05 mm. The zone has higher porosity and therefore lower strength and elastic properties. It has both lower strength and elastic modulus then cement paste. In Figure 9 the ITZ is shown in between the cement paste and the aggregate as well as the structure of the cement paste and ITZ.
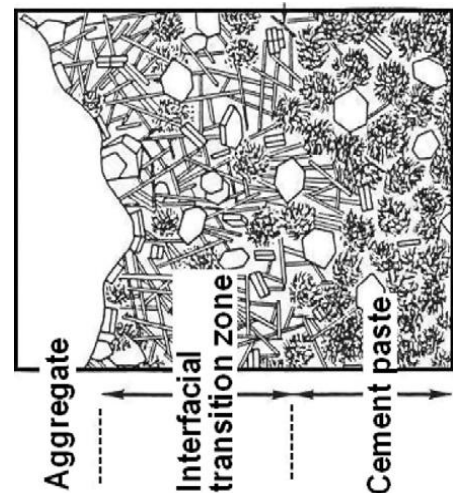
Figure 9: The interfacial transition zone between aggregate and cement paste [14].

Calculation methods for elastic modulus from characteristic strength

There are many models for estimating the elastic modulus from the characteristic strength of the concrete. Most standards give the elastic modulus as a function of the strength but some include the unit weight of the concrete. EuroCode 2 gives the evaluated elasticity using the characteristic compressive strength by the following equation [5]:

$$E_c = 22[(f_c)/10]^{0,3} \tag{12}$$

Where f_c is the measured ultimate compressive strength. The EC2 gives recommendations when using different types of aggregate, for limestone and sandstone reduction in elastic modulus is 10% and 30%, respectively. For basalt, an increase of 20% can be applied. In the Icelandic national annex for EC2 it is recommended; to be calculated as 10% reduction for normal porosity basalt and 40% for high porosity basalt.

American Concrete Institute committee 318 gives the following estimate [6]:

$$E_C = 4,73(f_c)^{1/2} \tag{13}$$

As the elastic modulus of SCC differs from that of conventional concrete the following equation:

$$E_C = 0,043\gamma_c^{1,5}\sqrt{f_c'} \tag{14}$$

Where γ_c is the unit weight of the SCC and f_c' is the specific strength [7].

If using high strength concrete a different empirical equations apply, CEB90 gives the following equation [8]:

$$E_C = 10(f_c + 8)^{1/3} \tag{15}$$

And the ACI committee 363 gives the following [9]:

$$E_C = 3,32(f_c)^{1/2} + 6,9 \tag{16}$$

All units of elastic moduli are given in GPa and all strength values are in MPa.

2.2.2. Models to estimate the elastic modulus of the concrete composition

Here, 5 types of models to estimate the elastic modulus of the concrete. These models all assume that the concrete is made of two composite elements, i.e. mortar and aggregate.

Parallel Model

The parallel model is based on the assumption that the elements, i.e. mortar and aggregate, are placed side by side. That means that the mortar and aggregate are subjected to the same amount of strain. This is shown in Figure 10. Following equation gives the estimated modulus:

$$\frac{E_C}{E_m} = 1 + \left(\frac{E_A}{E_m} - 1\right)V_A \tag{17}$$

Where E_C is the elastic modulus of the concrete, E_m is the modulus of the mortar and E_A is the modulus for the aggregate. And VA is the volume of aggregate. This model is also known as the Reuss´ model [10].

Serial Model

The serial model takes the mortar and aggregate as they are serial, i.e. they stack up. This is shown in Figure 10 and means that the elements are subjected to the same amount of stress.

$$\frac{E_m}{E_C} = 1 + \left(\frac{E_m}{E_A} - 1\right)V_A \tag{18}$$

The model parameters are the same as defined in the parallel model. This model is also known as the Vogits model.
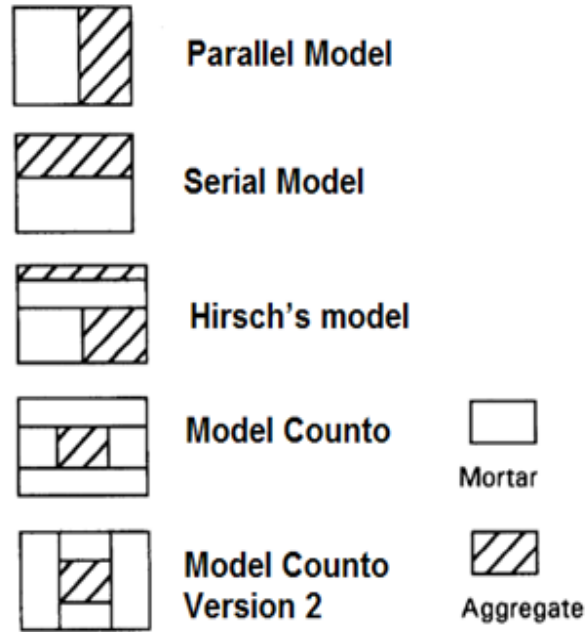
Figure 10: Composite Models

Hirsch's model

It has been shown that the parallel model overestimates the elastic modulus of the concrete and the serial model underestimates it. A combination of both Vogits and Reuss´ model can be expressed as follows:

$$\frac{E_m}{E_C} = \frac{1}{2}\left(\frac{1}{1 + \left(\frac{E_A}{E_m} - 1\right)V_A} + \left(1 + \left(\frac{E_m}{E_A} - 1\right)V_A\right)\right) \tag{19}$$

This model is named Hirsch's model[11], and shown in Figure 10(c).

Model Counto

Another way of combination of the models is Model Counto [12], it assumes the aggregate are wrapped in the mortar and the mortar calculated as serial. It is described by the following equation:

$$\frac{E_C}{E_m} = 1 + \frac{V_A}{\sqrt{V_A} - V_A + \frac{E_m}{E_A - E_m}} \tag{20}$$

Model Counto another version

Another version of the Model Counto, where the mortar is calculated as parallel, given by the following equation:

$$\frac{E_C}{E_m} = 1 + \frac{V_A}{\frac{E_A}{E_A - E_m} - \sqrt{V_A}} \tag{21}$$

Where in all cases E_C is the elastic modulus of the concrete, E_m is the modulus of the mortar and E_A is the modulus for the aggregate and V_A is the volume of the aggregate.

2.3 Creep behavior

2.3.1 Basics of creep behaviors

Creep is the tendency of solids to deform over time under constant stress. This means that the strain of a solid is increasing with time. All materials have this tendency to creep. This behavior is dependent on the degree of stress, time and temperature. The so called power-law will be used to describe the creep development. This development can be divided into 4 stages on a curve, strain vs. time [17, 18].

- Stage 1: Initial instantaneous strain
- Stage 2: is described by Andrade´s creep law were the strain depends on time, described as follows: $\varepsilon = \beta t^{1/3}$
- Stage 3: is the so called steady-stage creep development, described $\varepsilon = \kappa t$
- Stage 4: this is the final stage and is a stage of rapid creep development until failure
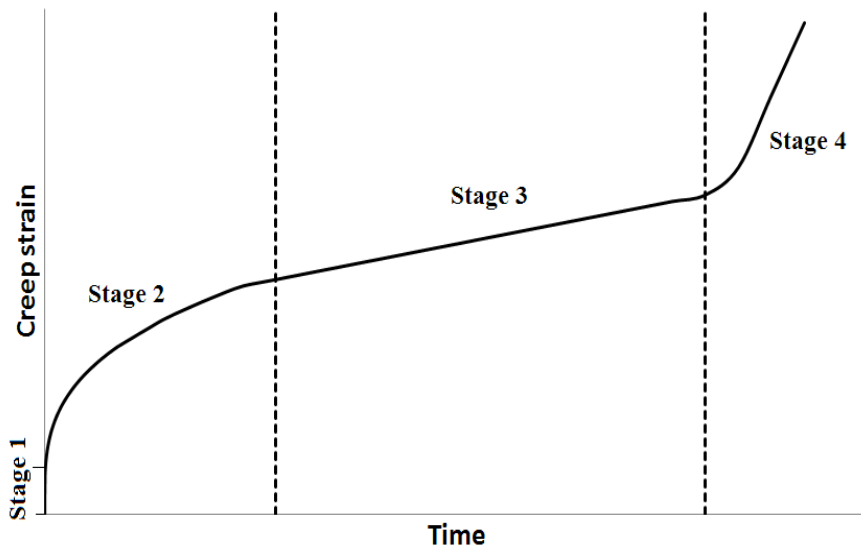
Figure 11: Creep development at diffrent stages

2.3.2 Concrete creep

Creep is the deformation of concrete over time under load, in other words it is the tendency of the concrete to slowly move (deform) under constant stress. The creep occurs as a result of long term exposure to high load and is highly dependent on temperature. The rate of creep is dependent on the time of loading (the age of the concrete when load is first applied), material properties and the duration that the concrete has been under load. Long term effects of creep are large deformations that can result in structural failure.
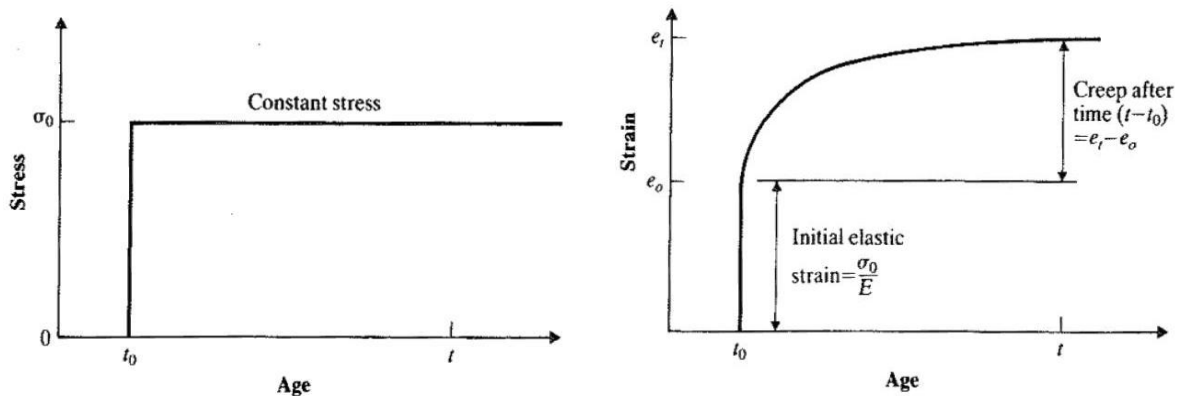
Figure 12: The graph to the left shows the stress over time for a concrete sample and the graph to right shows strain over time (both initial strain and creep strain)

Figure 12 shows the load function over time on the left and the tendency of the concrete to deform over time when the load is constant to the right. The rate at which the concrete deforms is significantly influenced by the concrete age at loading. If the concrete is loaded at early age the creep can be more than double compared to when it is loaded at 28 days, which is the normal practice. For example in EuroCode2, the creep function is expressed as a function of both the age of the concrete and the age of the concrete at loading. There are though other factors that influence concrete creep. The factors that influence the creep are the material properties of the concrete, the ambient relative humidity and the size of the section. [19]

Concrete creep can be categorized into two types of creep; basic creep and drying-creep. Basic creep is the deformation of a concrete samples without any moisture exchange, that is the sample is completely isolated from the environment and kept at constant humidity and constant temperature. Drying creep is the total deformation of the sample when it is not isolated from the environment; that is the moisture exchange is allowed to take place. One would assume that the difference in deformation between the basic creep and drying creep should only be the shrinkage deformation, but that is not true. Drying creep is always more than the combined effect of shrinkage and base-creep. This difference is named "The Pickett effect" after the man who discovered it, Gerald Pickett [20, 21]. A schematic picture of this can be seen in Figure 14 [22].

It is impossible to separate the deformation of concrete completely, e.g. between creep, shrinkage or deformation because of heat difference. So when researching these effects the samples are cast simultaneously and kept under different conditions. To investigate creep, shrinkage samples are also cast and thus creep and shrinkage are then measured at the same time. The samples are kept at constant temperature and constant humidity, the only difference is that the creep samples are under constant load. So when calculating the creep the difference in

deformation needs only to be measured. For further explanation, the following equation is presented:

$$c = \varepsilon - \frac{\sigma}{E} \pm S_h \pm S_T \qquad (22)$$

Where c stands for creep, ε for total deformation, S_h for shrinkage and S_T for deformation due to temperature changes. Concrete creeps under load as earlier discussed, but when the load is removed there is a recovery of deformation. This is explained by Figure 13 where it can be seen that the elastic deformation is partly recoverable. The elastic deformation is not totally recovered as the cement has been reacting over time which results in higher young-modulus. The rest of the deformation is creep but over time there is also a recovery in creep. The difference in basic creep and drying-creep are also shown in Figure 13. It should be noted that creep is interlinked to shrinkage and when observing creep, shrinkage should be observed as well.
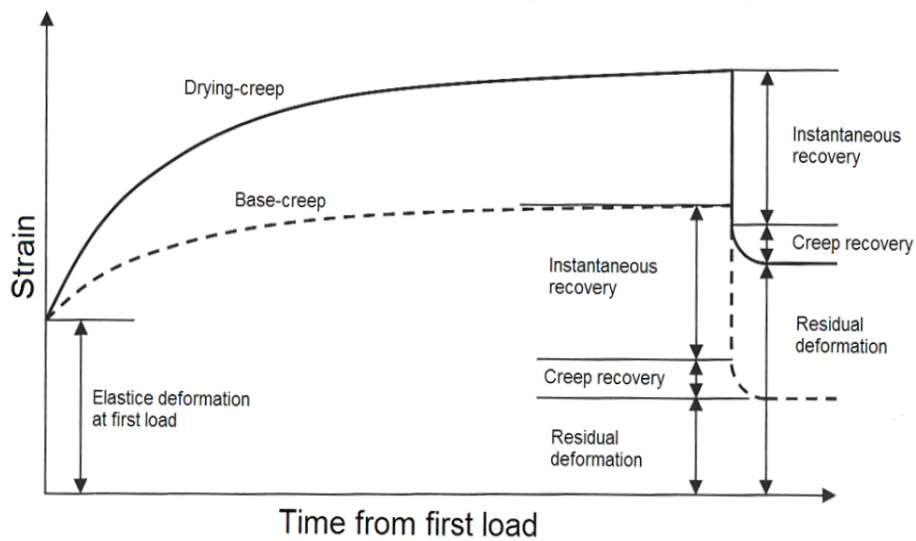
Figure 13: The deformations of the concrete when load is applied and then removed. It shows graphs for both samples that are stored under wet and dry conditions [23]
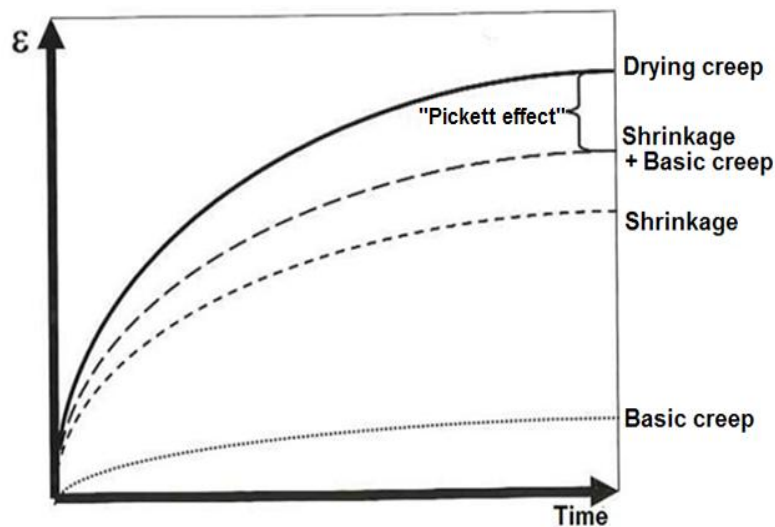
Figure 14: The relative effects of shrinkage and creep of normal concrete, in addition to the so called "Pickett" effect [20]

The Pickett effect (Drying creep)

The drying creep, also referred to as the Pickett effect, is the creep increase when the specimen undergoes drying. The interpretation of the extra deformation and its mechanism has been a controversial topic for more than 60 years. Many hypotheses have been presented by many researchers and there are two major views that exist in the literature about the Pickett effect. One hypothesis explains the extra deformation by a mechanism explained by shrinkage-induced stress and associated cracking [24, 25]. The other considers the real mechanism by which creep interacts with drying [26, 27]. But neither of these views explains the phenomena fully so a combination of both views has prevailed in the literature.

Today the mechanism of drying creep is considered to be the combination of at least two components, i.e. the sum of the both. The first component is intrinsic drying creep with its own mechanism [28]. The seconded is a structural drying creep caused by micro-cracking effect due to the non-uniformity of the drying of the specimen. To be accrued there appear to be two major mechanisms that cause the Pickett effect, the micro cracking and the stress induced shrinkage.

The micro cracking is caused when there is a shrinkage gradient through the section of a specimen where there is more shrinkage on the surface then in the inner layer of the specimen. This causes tension on the surface which causes micro cracking, i.e. restrained cracking. Due to the nonlinear inelastic behavior of the concrete creep caused by tension, the micro cracks cannot fully close when the
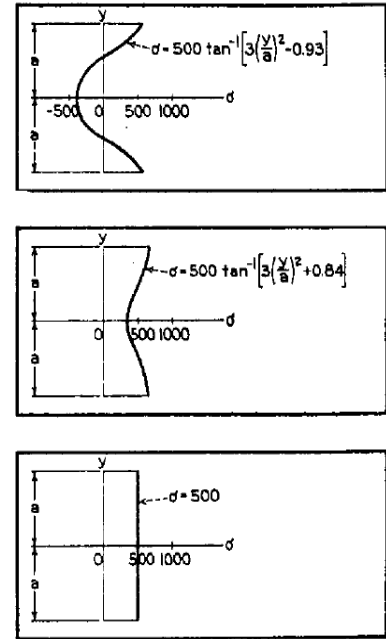
Figure 15: Moisture distribution over a concrete element [21]

moisture distribution finally approaches a uniform state, see Figure 15. Consequently, the true shrinkage is always more than the shrinkage of drying specimen. There is more shrinkage in the loaded specimen then the free shrinkage specimen, which can falsely be considered as creep. Shrinkage in loaded specimens has been observed to be more than in unloaded specimens [29].

The stress-induced shrinkage mechanism has been defined by detailed analysis of creep data by Bazant and Chern [26], there it is explained differently. There exist two types of moisture diffusions, i.e. macro-diffusion and micro-diffusion. Macro-

Figure 16: Typical strain for different types of testing[26]

diffusion is the movement of moisture between and through the large pores, it has no measurable effect on the deformation. Micro-diffusion is the movement of moisture between the capillary pores and gel pores. The Micro-diffusion affects the deformation rate of the solid framework of the cement gel. The movement of water through the gel pores increases the rebounding and debounding processes that are the source of creep [29].

In testing when the samples are moist covered the Pickett effect is eliminated because the shrinkage is suppressed and by this the basic creep is isolated. Unlike the moist covered the Picket effect can be observed in the sealed and drying samples. Internal drying occurs in the sealed samples, where as in the drying concrete there is both internal and external drying. In all prospective the different mechanisms of the Pickett effect are likely included. Typical results for these three types of testing are shown in Figure 16 [30].

2.3.3 Theories concerning the mechanisms of concrete creep

Consolidation theory

Consolidation theory was proposed in 1985 by M. Ortiz [31] and is based on research on inelastic behavior of the concrete [32]. The theory has three basic requirements that the author presents; 1. The theory should be based on the first principle of mechanic, 2. it should be appropriate for use in computation and 3. be accurate in reproducing a broad range of experimental data. There is a lot of evidence that point to the conclusion that there are two main mechanisms that influence the inelastic behavior of concrete. Firstly, the extension of microcracks in concrete which are known to play a vital role in inelastic behavior. Secondly Slip-type plastic flow[33].

It has been observed that when samples are subjected to uniaxial compression stress, they will develop cracks in load direction [34]. This means that that the cracks in concrete can open against compression stress, which disagrees with the second law of thermodynamics that requires that cracks open under tension. This can although be considered to be somewhat simplified as concrete is not a homogenous material. In the theory of inelastic behavior of concrete [32] it is proposed that concrete is comprised of two phases; mortar and aggregate. This gives the application of difference in applied stresses in the phases. This can also give an explanation into the

Figure 17: Interaction between aggrgate and morter of a concrete mass [31]

transversal stresses in the concrete mass. As can be seen in Figure 17 when the compressive stress σ is applied to the concrete mass, there is an interaction between aggregate. This results in tension stress in the mortar (the matrix that adhesively binds the aggregate) which explains the

cracks in load direction. The proposed theoretical model assumes that the inelastic behavior of the concrete is due to the following factors:

- The material behavior of the mortar
- The material behavior of the aggregate
- And the interaction between the two

This implies that concrete is taken as a composite material, composed of mortar and concrete. To model each part independent models for the composite material will be introduced. First a damage model for the mortar is modeled, in [32] the Gibson energy for a brittle martial with continues micro-cracking is introduced and is defined as follows:

$$G = \frac{1}{2}\boldsymbol{\sigma}:\boldsymbol{C}:\boldsymbol{\sigma} - A^c \tag{23}$$

Where $\boldsymbol{\sigma}$ is the stress tensor, $\boldsymbol{C}$ is the elasticity tensor of the material and A^c is the free energy to form micro-cracks, the symbol (:) donates the dyadic product for the tensor calculations. It should be noted that this is a formulation for the mortar and as such the stress donated by $\boldsymbol{\sigma}$ can differ significantly from the exactly applied one, as the mortar is a component of the concrete. By applying the stress-strain relationship corresponding to the form of energy potential:

$$\varepsilon = \frac{\delta G}{\delta \boldsymbol{\sigma}} = \boldsymbol{C}:\boldsymbol{\sigma} \tag{24}$$

The elastic rate of deformation is then:

$$\dot{\varepsilon} = \boldsymbol{C}:\dot{\boldsymbol{\sigma}} + \dot{\boldsymbol{C}}:\boldsymbol{\sigma} = \dot{\varepsilon}^c + \dot{\varepsilon}^i \tag{25}$$

Where $\dot{\varepsilon}^c$ is the elastic rate of deformation that would be obtained by preventing the micro-cracking to extend further and $\dot{\varepsilon}^i$ is the rate due to the degradation of the elastic properties. It is though assumed that *"the values of the elastic compliances themselves be taken as the characterization of the state of damage of the material"* [32]. So the elastic compliances tensor can be divided into two structures:

$$\boldsymbol{C} = \boldsymbol{C^0} + \boldsymbol{C^c} \tag{26}$$

Where $\boldsymbol{C^0}$ is the elasticity tensor of the uncracked material and the tensor $\boldsymbol{C^c}$ is to take into account the increased flexibility due to active micro-cracking (due to cracks that are in the process of opening). The deformation is then obtained:

$$\varepsilon = (\boldsymbol{C^0} + \boldsymbol{C^c}):\boldsymbol{\sigma} = \varepsilon^0 + \varepsilon^c \tag{27}$$

Where $\boldsymbol{\varepsilon^0}$ is the deformation occurring in the absence of micro-cracking and $\boldsymbol{\varepsilon^c}$ is the deformation because of micro-cracking. If the micro-cracks remain closed due to compressive stress they do not contribute to the deformation $\boldsymbol{\varepsilon^c}$. To eliminate this element the deformation $\boldsymbol{\varepsilon^c}$ is conditioned to have positive eigenvalues. By further formulation given in [31] it can be concluded that the Gibbs potential is given by:

$$G = \frac{1}{2}(\boldsymbol{\sigma}:\boldsymbol{C^0}:\boldsymbol{\sigma} + \boldsymbol{\sigma^+}:\overline{\boldsymbol{C}}^c:\boldsymbol{\sigma^+}) - A^c \tag{28}$$

Where $\boldsymbol{\sigma^+}$ is the positive part of the stress tensor $\boldsymbol{\sigma}$ and $\overline{\boldsymbol{C}}^c$ represents the extra flexibility obtained if all the micro-cracks would be active. If the micro-cracks form in sick-sack, described as the cross effect, it can be active in two modes. The first is when the crack is splitting and is called the splitting mode, the other is the compressive mode where the cracks become active in compression due to the sick-sack dimensions of the micro-crack. To take this into account the elasticity tensor $\overline{\boldsymbol{C}}^c$ is divided into two parts, one for each mode.

$$\overline{\boldsymbol{C}}^c = \overline{\boldsymbol{C}}_I^c + \overline{\boldsymbol{C}}_{II}^c \tag{29}$$

To get further information on this see [31].The part of the aggregate has to be taken into account as well as the mortar. Aggregate are into the formulation of the theory by simple model, a criteria which is frequently used to characterize the failure of the choosiness soils [35].

$$\Phi(\boldsymbol{\sigma}) = q - Mp \tag{30}$$

The Solidification theory

Concrete creep is influenced in a profound way by the hydration processes of the cement. This influence which is also known as aging is the factor that causes concrete creep under constant stress to decrease as the age of loading increases. This effect occurs throughout the entire life of the concrete and does not only affect young concrete. Modeling of these influents has proven to be a major complication. In this chapter there is a short formulation of the solidification theory which was developed by Z.P. Bazant and S. Presana [36]. This theory has the function of eliminate the short comings of the former formulations of the aging effect. The following formula is a micromechanics-based creep model for solidifying material:

$$\varepsilon = \frac{\sigma}{E_0} + \varepsilon_c + \varepsilon_0 \tag{31}$$

Where ε is the total strain, σ is the constant stress, E_0 is the Young´s modulus, ε_c is creep strain and ε_0 is the sum of hygrothermal strain (drying shrinkage, thermal dilatation, autogenous shrinkage and cracking strain (when under high stress)). The creep strain is defined as the sum of viscoelastic strain ε_v and viscous strain ε_f:

$$\varepsilon_c = \varepsilon_v + \varepsilon_f \tag{32}$$

At high stress both ε_v and ε_f become nonlinear and then they represent viscoelastic-plastc strain and the viscoplastic strain.

The theory assumes the elastic modulus is constant over the age of the concrete but commonly it is assumed that the modulus is dependent on age, i.e. it is assumed that the elastic modulus changes as the concrete gets older. This is to make the formulation of the theory less complex and if the elastic modulus is age-dependent it is a complication is unnecessary and

thermodynamically objectionable. Also the elastic modulus E_0 is a material constant and is defined as <u>asymptotic</u> modulus.

In Figure 18 there is a rheological model that reflects the accumulation of strain represented in eq. (31). The model describes the ageing as a consequence of growth of the volume fractions v and f of solidifying hydrated cement which are associated with the viscoelstic and viscous strains, respectively. The growth of these two fractions where mathematically formulated by Bazant [37, 38, 39].
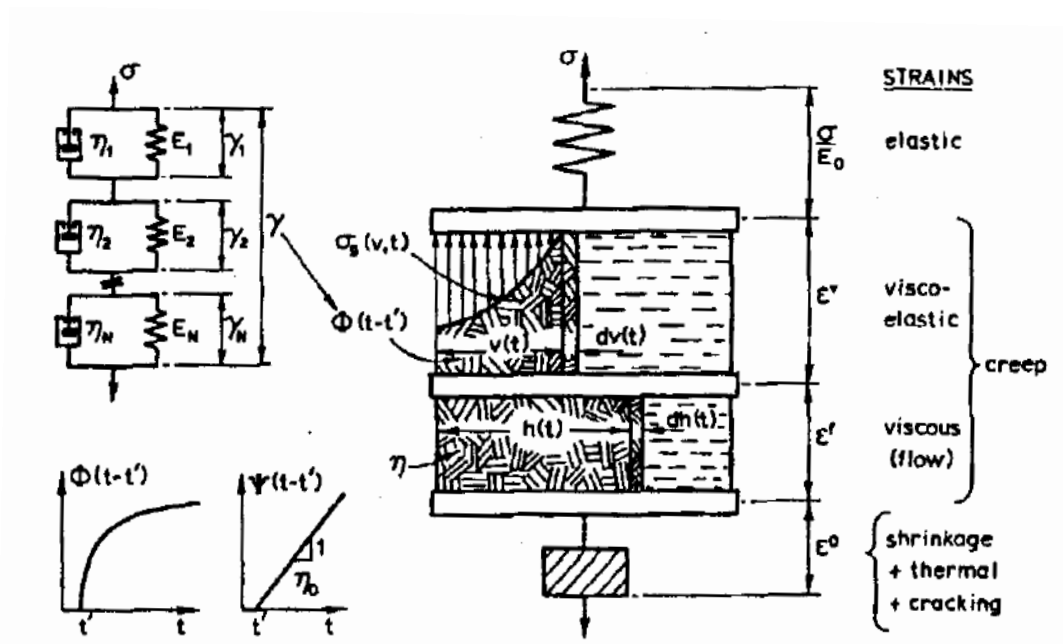
Figure 18: Rheological model reflection accumulative strain from all parts strains, elastic strain, creep strain and hygrothermal strain [36].

Colloid model for concrete creep and shrinkage

This is the model developed by Jennings and discussed in [40]. It is a model for the calcium silicate hydrate (C-S-H) structure on nanometer level. The model describes the C-S-H gel as group of solid particles which are colloid size. This model was developed to attempt to account for many physical attributes of mature C-S-H paste, such as particle size, density, surface area and pore´s structure. But one of the main emphases in this will be the ability of the model to describe/hypotheses the mechanism of viscous flow under load and under drying conditions. Aging, which is for example a large factor in creep development, is defined as the increase of hydration products over time, so as for the model this is described as there become more connections between globule particles which in fact increases the density of the C-S-H structure and makes it stiffer and stronger. The hypotheses proposed by Jennings suggests: that the small globule particles move and reposition them self's with time when the C-S-H structure is subjected to constant load or drying [40].
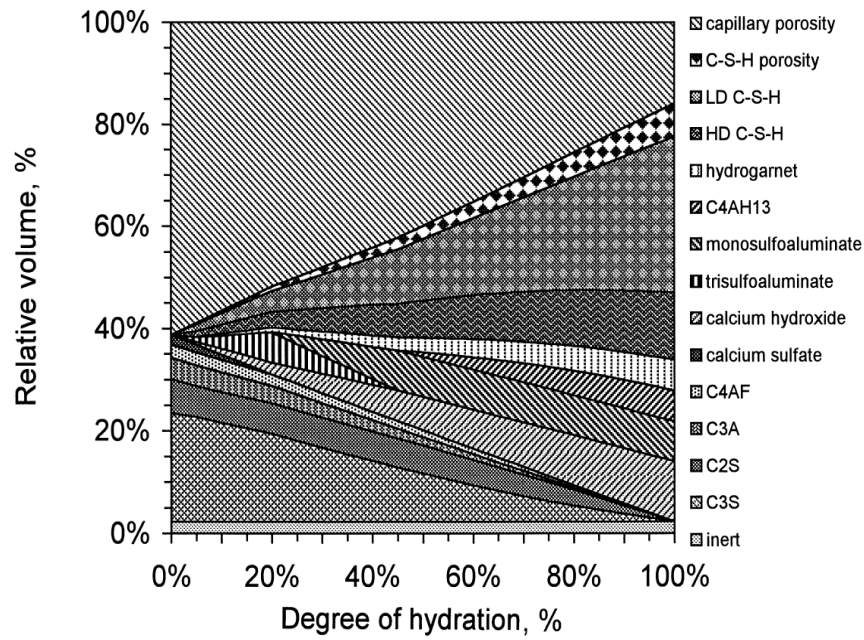
Figure 19: Relative volume of each phase as a function of the degree of hydration [41].

The model assumes two types of densities of the C-S-H particles. These two types are the low density calcium silicate hydrate (LD C-S-H) and high density (HD C-S-H). The difference of these densities is that one can be observed by N_2 (nitrogen gas) and the other cannot. The cement past contains more than one component so one of the main problems is to determine the amount of C-S-H in the past. The model assumes as simple stoichiometric reaction of the main cement reactants, that is C_3S, C_2S, C_2A and C_4AF, see Figure 19. For more information on this see [40, 41, 42].

2.4   Shrinkage of concrete

Shrinkage in concrete is a deformation that takes place when there is no static load applied. The main reason for shrinkage is because of water leaving the concrete. This means less water is in the small porous veins in the concrete. This makes the concrete contract because the pressure in the veins has decreased and is lower than the atmospheric pressure which causes shrinkage. It could be stated that this is caused by two main things. Firstly, because of a difference in relative humidity between the concrete and the surroundings, water vaporizes from the concrete. Secondly, because the concrete uses water in the reaction process (while curing) the volume of water decreases; the total volume decrease of the cement paste is about 11% [23]. Shrinkage can be categorized into a few types. The main categories are plastic shrinkage, chemical shrinkage, drying shrinkage, autogenous shrinkage and carbonation shrinkage [23].

Plastic shrinkage

Plastic shrinkage takes places shortly after casting when the concrete starts to harden. This occurs because water vaporizes and also reacts with the cement. When this happens there is a change in volume and the concrete shrinks. This can often leave large distinct cracks on the

Figure 20: How plastic shrinkage cracks the surface of concrete that is hardening

surface of the concrete. At this point the concrete is no longer a liquid but hasn't got any significant strength yet either [23].
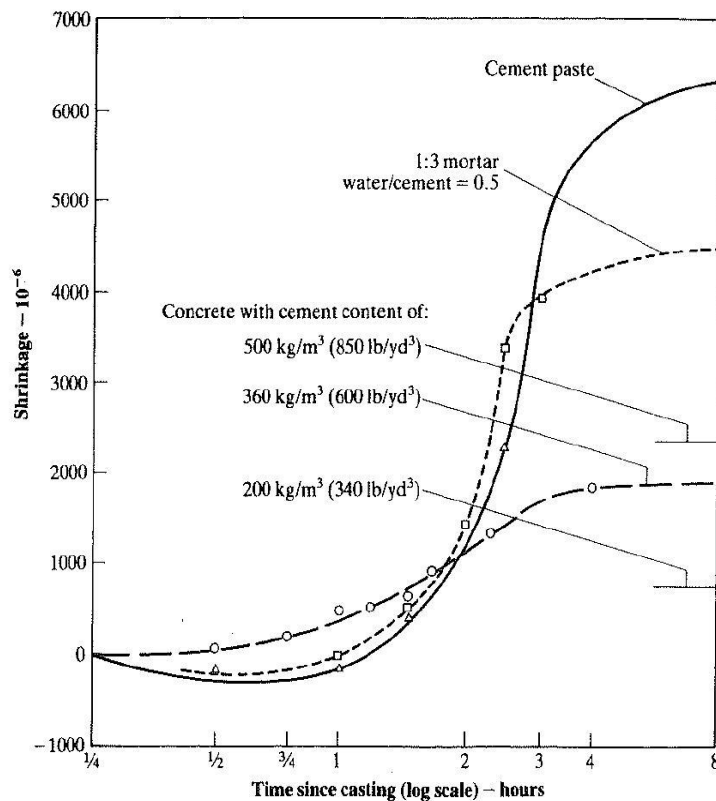
Figure 21: Influence of cement content on the plastic shrinkage at a temperature of 20 °C, relative humidity of 50% and wind speeds of 1 m/s [20]

Plastic shrinkage can be defined as the volumetric contraction of the cement past. As the cement paste is plastic it undergoes this contraction which is about 1% of the absolute volume of dry cement. The contraction is caused by the loss of water by evaporation from the surface of the concrete. It can also happen when there is suction from dry concrete from below. This volumetric contraction creates tensile stresses in the surface layer of the concrete as there are close to no volumetric changes deeper into the concrete, and as the concrete is in its plastic stage, it is very weak. Therefore plastic cracking occurs at the surface [20]. A schematic picture of this is

shown in Figure 20.

Plastic shrinkage becomes greater as the evaporation rate of water increases; this of course depends on the relative humidity in the air and the wind speed. ACI 305R-99 recommends that a evaporation rate greater then 0,25 kg/h/m^2 should be avoided to prevent cracking of the surface. So to reduce plastic shrinkage the evaporation can be completely prevented immediately after casting. As the cause of plastic shrinkage is the loss of water from the cement past it is highly dependent on cement content; this can be seen in Figure 21 [20].

Chemical shrinkage

Chemical shrinkage takes place while the water and cement are reacting. This occurs fastest in the beginning when the water and cement are combined but slows down as more of cement has

reacted. When this reaction is taking place many chemical compounds are created but mostly the CSH-gel. The CSH-gel that is created in the process has less volume then the cement before the reaction. This makes the concrete shrink. This type of shrinkage is evenly distributed over the total section and not localized to the surface, like other types of shrinkage [23].

Autogenous shrinkage

Autogenous shrinkage occurs in combination with chemical shrinkage, it was first discussed in 1934 by Lymen [43]. The water the cement uses for the reaction comes from the pores and small veins in the concrete. As the water leaves the veins there is a loss of pressure in the same way as in the drying shrinkages. This happens in spite of drying out, that is if the concrete is drying out or not [23]. In conventional concrete this shrinkage is typically very small, about 50×10^{-6} to 100×10^{-6}, but can be greater in high performance concrete [20, 44].

Drying shrinkage

Drying shrinkage occurs after the setting-process, when the concrete is hardening. This type of shrinkage is most effective when the concrete is young and decreases as the concrete gets older. This is very dependent on external conditions, e.g. relative humidity, temperature and wind. If the concrete is located were the relative humidity is less in the environment than in the concrete itself, it dries out and water dissipate from the porous veins in the concrete. This lowers the pressure in the pores and the concrete shrinks. Drying shrinkage often creates subtle network of cracks on the surface of the concrete [23].

When water evaporates from hardened concrete stored in unsaturated air it causes drying shrinkage. Some part of this shrinkage is irreversible and has to be distinguished from the reversible part which is moisture movement. The left part in Figure 22 shows how a sample that has been drying in unsaturated conditions is put into water, and shows the swelling when cement absorbs water. When it is then made to dry again the drying shrinkage begins once more, this can be done repeatidly and then the recovery of shrinkage will become increasingly less.
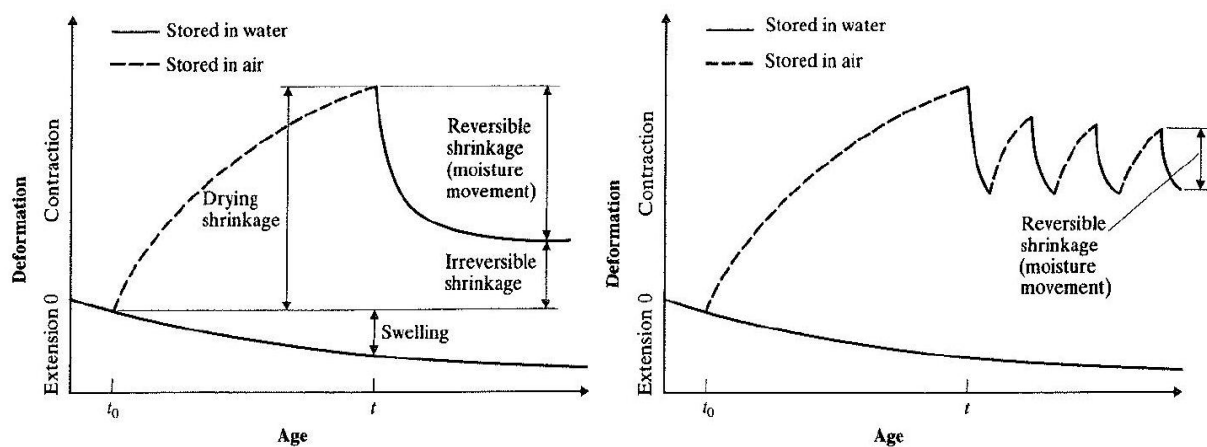
Figure 22: Moisture movement in concrete; the left graph shows data for concrete which has dried from t_0 to t and then re-saturated, the right graph is for concrete that has dried from t_0 to t and subjected to cycles of wetting and drying [20]

38

This can be seen in left part of Figure 22. The reversible part of the drying shrinkage is about 40% to 70%, this depends on the age of the concrete when drying was first commenced, e.g. if concrete is allowed to fully hydrate before it is exposed to drying the reversible part of the drying shrinkage is greater. The irreversible part of the drying shrinkage is associated with the forming of new physical and chemical bonds in the cement when water is removed. When concrete dries there is a loss of free water, i.e. the water in the capillaries which is not bound. This creates internal relative humidity gradients in the cement paste which transfers the water molecules from the large surface area of the calcium silicate hydrates into empty capillaries and finally out of the concrete. This makes the cement paste contract but the reduction in volume is not the same as the reduction from water that was removed. This is because of the initial loss of free water has significantly lower effect on volumetric contraction and also because of the initial restraint to consolidation by the calcium silicate hydrate structure [20].

2.5   Aggregate and there effects on concrete creep

Aggregate are one of the main ingredient of a concrete mix and make up around 65%-80% of the mixture. Aggregate can be of all sorts, but are categorized into two main types; the coarse aggregate (e.g. gravel, crushed aggregates) and fine aggregate (e.g. river sand). Aggregate can be made of main types of rock materials, such as basalt, granite, limestone or even sandstone. Although the different types of rock have varied properties they essentially fulfill the main role of the aggregates, i.e. to fill the void between the cement matrix to create concrete.

Weight to volume relationship

In this section there will be a short description on the weight to volume ratios and calculation methods for e.g. unit weight, porosity and water absorption. First the volume and the weight need to be defined for the material, in Figure 23 there is a representation of the part of the material, i.e. solid part, water part and air part. The following can be formulated from the setup presented in Figure 23:

$$V = V_s + V_v \tag{33}$$

Here V is the total volume of the unit, V_s is the volume of the solid materials and V_v is the volume of the voids. Void volume is the volume of both water and air in the unit and can be formulated as follows:

$$V_v = V_w + V_a \tag{34}$$
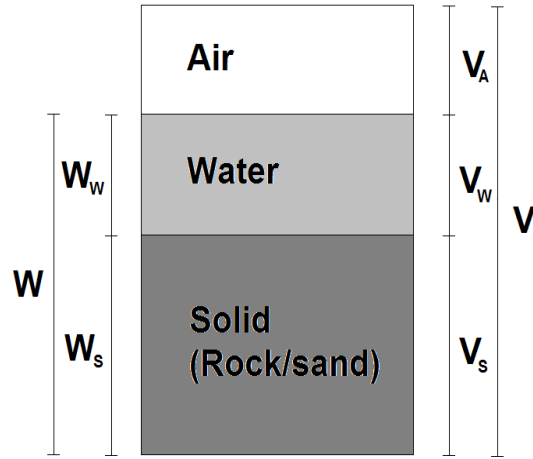
Figure 23: Volume ratio and weight ratio of a section of material

The weight of this

$$W = W_s + W_w \tag{35}$$

$$e = \frac{V_v}{V_s} \tag{36}$$

$$n = \frac{V_v}{V} \tag{37}$$

$$w = \frac{W_w}{W_s} \tag{38}$$

From these definitions and more defined in [45]

$$n = \frac{\omega_{sat}}{(1 + \omega_{sat})} \frac{\rho_{SSD}}{\rho_w} \tag{39}$$

Where ω_{sat} is the water absorption, ρ_{SSD} is the density of the aggregate under saturated surface dry conditions, and ρ_w is the density of water [45].

Aggregates and concrete creep

It is assumed that most of the creep is because of deformation in the paste. One of the main reasons is movement of water in the smallest pores, so called gel pores, also movement of water from the gel pores and through the small capillaries of the paste [46].
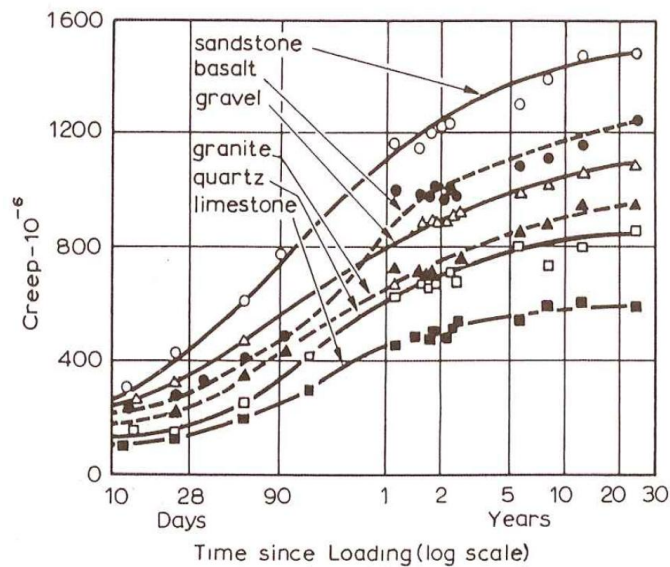
Figure 24: Difference in creep for concrete with variation of aggregates [23]

Some properties of aggregates affect the creep of concrete. Porosity of the aggregates affects the young-modulus and water absorption and thus affects indirectly the creep. More dense aggregates means less porosity, thus less creep. Probably the most crucial factor in creep development is the young-modulus; the greater the young-modulus the less creep there is [20]. If the aggregates have lower young-modulus the greater the stress on the concrete paste becomes and thus the creep becomes more. Long-term effects of aggregates on creep are less known than the short-term effects. There have been some studies on the effect of different types of aggregates. One of these studies is shown in Figure 24. It can be seen that the concrete made with basalt is quite different from the other aggregates. On day 90, the creep rate increases a lot compared to the other aggregates. At the age of one year the creep rate decreases again and the rate becomes similar to the other aggregates [23].

Creep of aggregates
Stone materials are known to creep [47, 48, 49], as is for most materials, they slowly densify under pressure over time. This movement slows down with time, most often logarithmically. The creep of rock material is often around 0,2-0,4 mm/m under a load approximately 20 MPa for about 4 days. For marble silica the creep of the material has been observed to be 0,12 mm/m under 80 MPa load and it has been shown that the secondary creep increases with increased loading [50].

The effects of aggregates on concrete shrinkage
Aggregates are a large part of the concrete mix or 60%-80% and their effects on shrinkage have been studied by many. The elastic modulus (young-modulus) effects the concrete in many ways and concrete made with lightweight aggregates has exhibited higher shrinkage than conventional concrete made with normal weight aggregates. Even in the range of normal weight aggregates

41

there is a lot of variation in shrinkage behavior because of variations in the young-modulus [20]. The difference in shrinkages for various types of aggregates can be seen in Figure 25.
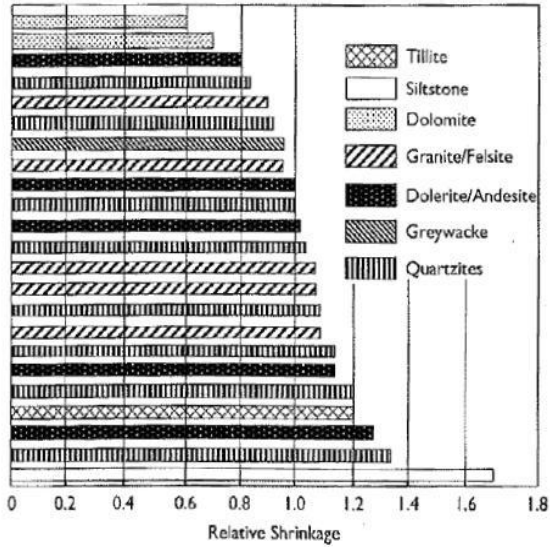
Figure 25: Effect of various aggregates on shrinkage [51]
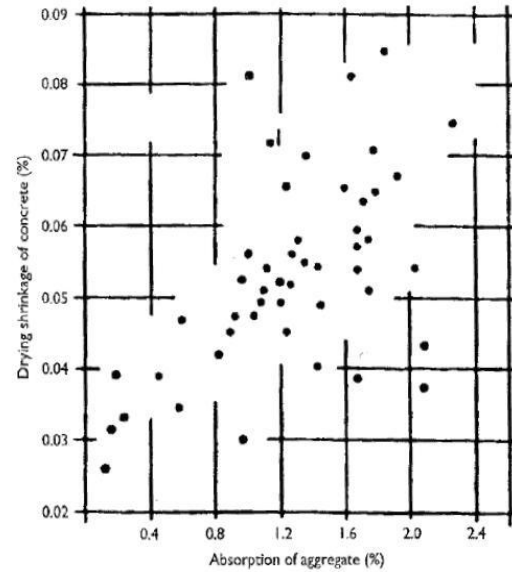
Figure 26: Effects of different absorption % on the drying shrinkage [51]

Of course the porosity of the aggregates affects the Young-modulus and the absorption of the aggregates. There have been studies on how the absorption affects the concrete shrinkage; this can be seen in Figure 26. Here it can be pointed out that the graph only goes up to 2,4%, but Icelandic porous aggregates are commonly in the range of 3%-7%.

2.6 Modeling of both concrete shrinkage and creep

2.6.1 The Creep and shrinkage models of EuroCode 2

Most code equations for the EC2 attributes creep and shrinkage of concrete to the relative humidity, dimension of the element, and composition of the concrete. It also states that creep is influenced by the maturity of the concrete when the load is first applied and depends on duration and magnitude of the sustained load.

Creep is calculated using a creep coefficient $\varphi(t, t_0)$ which relate to the tangent stiffness modulus (E_c) of the concrete. The creep deformation of the concrete can be estimated using the creep coefficient as follows:

$$\varepsilon_{cc}(t, t_0) = \varphi(t, t_0) \cdot \frac{\sigma_c}{E_c} \tag{40}$$

where the creep coefficient is defined as follows:

$$\varphi(t, t_0) = \varphi_0 \, \beta_c(t, t_0) \tag{41}$$

The t value corresponds to the time of observation and t_0 is the age of the concrete at the time of loading. Also φ_0 is the notional creep coefficient, and the method to calculate is described in

42

Annex B in the EC2 [52]. The notional creep coefficient takes into account the ambient relative humidity, strength class of the concrete, and concrete age at loading. The time coefficient $\beta_c(t, t_0)$ can be calculated as follows:

$$\beta_c(t, t_0) = \left[\frac{(t - t_0)}{\beta_H + t - t_0}\right]^{0,3} \tag{42}$$

In EC2 the total shrinkage is divided into drying shrinkage and autogenous shrinkage, shown in the following equation:

$$\varepsilon_{cs} = \varepsilon_{cd} + \varepsilon_{ca} \tag{43}$$

Where ε_{cs} is the total shrinkage and ε_{cd} and ε_{ca} represent the drying shrinkage and the autogenous shrinkage accordingly. The drying shrinkage is expressed as follows:

$$\varepsilon_{cs} = \beta_{ds}(t, t_s) \cdot k_h \cdot \varepsilon_{cd,0} \tag{44}$$

Where k_h is a coefficient dependent on the notional size h_0. The value for unrestrained shrinkage $\varepsilon_{cd,0}$ can be found in Table 1. The factor $\beta_{ds}(t, t_s)$ takes into account the age of the observed specimen.

Table 1: The value for $\varepsilon_{cd,0}$ for different strength classes and ambient relative humidity

$f_{ck}/f_{ck,cube}$ (MPa)	Relative Humidity (%)					
	20	40	60	80	90	100
20/25	0,62	0,58	0,49	0,30	0,17	0,00
40/50	0,48	0,46	0,38	0,24	0,13	0,00
60/75	0,38	0,36	0,30	0,19	0,10	0,00
80/95	0,30	0,28	0,24	0,15	0,08	0,00
90/105	0,27	0,25	0,21	0,13	0,07	0,00

The notional size is calculated as follows:

$$h_0 = \frac{2A_c}{u} \tag{45}$$

Where A_c is the concrete cross-section area and u is the perimeter for the part of the cross-section that is exposed to drying. Also the factor $\beta_{ds}(t, t_s)$ is defined as followes:

$$\beta_{ds}(t, t_s) = \frac{(t - t_s)}{(t - t_s) + 0,04\sqrt{h_0^3}} \tag{46}$$

Here t (in days) is for the age of the concrete which is being considered, t_s (in days) is the age of the concrete when it was first exposed to drying (normally at end of curing) and h_0 is the notional size as before.

The autogenous part of the shrinkage is defined as follows by the standard:

$$\varepsilon_{ca}(t) = \beta_{as}(t) \cdot \varepsilon_{ca}(\infty) \tag{47}$$

The so called final autogenous shrinkage is calculated from the compressive strength:
$$\varepsilon_{ca}(\infty) = 2{,}5(f_{ck} - 10) \cdot 10^{-6} \tag{48}$$

And the factor $\beta_{as}(t)$ is given as a function of time t (in days)
$$\beta_{as}(t) = 1 - e^{-0{,}2\sqrt{t}} \tag{49}$$

2.6.2   The Creep and shrinkage models of ACI209

The measured creep data was also compared to values predicted from The ACI 209 model [53]. The ACI 209 code uses the following factors to predict creep and shrinkage: the age at loading (la), ambient relative humidity (λ), the surface to volume ratio (vs) (or average thickness of specimen (h)) , slump of fresh concrete (s), fine aggregate percentage (ψ), cement content (c), air content (α), and curing period of the concrete (cp). The ACI 209 takes these aspects into account using correction factors which are applied to measured or suggested values. In the absent of measured values the suggested values (ultimate values) are as following:

$$\nu_u = 2{,}35\gamma_c \tag{50}$$

$$(\epsilon_{sh})_u = 780\gamma_{sh} \; x \; 10^{-6} \tag{51}$$

The factors γ_c and γ_{sh} take into account deviation from the standard condition, such as exposure time, time of loading, consistency, air-content, environmental conditions, content of fines, the size effect and content of cement. The equations for these factors are expressed as follows:

$$\gamma_c = \gamma_{c,la} \cdot \gamma_{c,\lambda} \cdot \gamma_{c,vs} \cdot \gamma_{c,s} \cdot \gamma_{c,\psi} \cdot \gamma_{c,\alpha} \tag{52}$$

$$\gamma_{sh} = \gamma_{sh,cp} \cdot \gamma_{sh,\lambda} \cdot \gamma_{sh,vs} \cdot \gamma_{sh,s} \cdot \gamma_{sh,\psi} \cdot \gamma_{sh,c} \cdot \gamma_{sh,\alpha} \tag{53}$$

Where $\gamma_{c,la}$ is factor to take into account the difference in loading age, and is defined as follows for moist cued concrete:

$$\gamma_{c,la} = 1{,}25(t_{la})^{-0{,}118} \tag{54}$$

Here t_{la} is the age at loading. The factor $\gamma_{sh,tc}$ takes into account the curing and exposure time. This factor is calculated from curing time and is expressed in the following formula:

$$\gamma_{sh,cp} = 1{,}202 - 0{,}2337 \log t_c \tag{55}$$
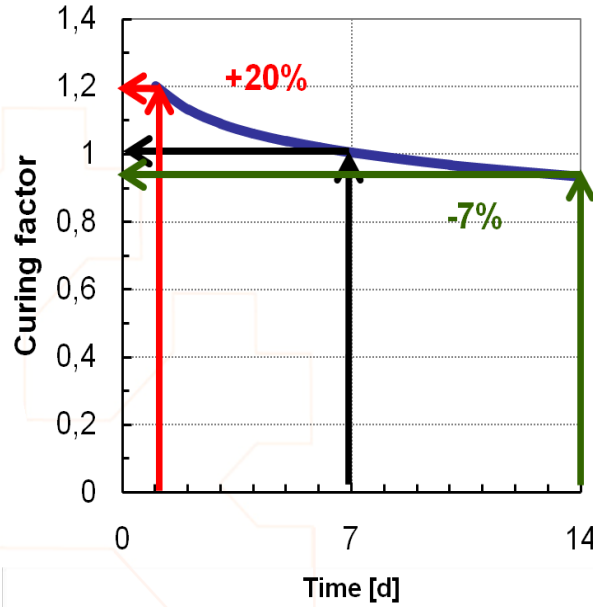
Figure 27: The difference in curing factor with time

In Figure 27 the development of the curing factor over time is shown, where the factor is 1,0 at seven days of curing. The factors $\gamma_{c,\lambda}$ and $\gamma_{sh,\lambda}$ take into account the effects of the environment, i.e. relative humidity.

$$\gamma_{c,\lambda} = \begin{cases} 1,0 & \lambda \leq 40 \\ 1,27 - 0,0067\lambda & \lambda > 40 \end{cases} \tag{56}$$

$$\gamma_{sh,\lambda} = \begin{cases} 1,0 & \lambda \leq 40 \\ 1,4 - 0,0102\lambda & 40 \leq \lambda < 80 \\ 3,0 - 0,03\lambda & 80 \leq \lambda < 100 \end{cases} \tag{57}$$

Where λ is the relative humidity in percent.

The size factors $\gamma_{c,vs}$ $\gamma_{sh,vs}$ takes into account different sizes of samples, the different in thickness. This can be expressed as follows:

$$\gamma_{c,vs} = \frac{2}{3}\left[1 + 1,13e^{-0,0213\,(V/S)}\right] \tag{58}$$

$$\gamma_{sh,vs} = 1,2e^{-0,0472\,(V/S)} \tag{59}$$

Where V is the volume and S is the surface area exposed to drying, V/S is in mm. This factor can also be calculated from the thickness of the structural element. $\gamma_{sh,s}$ is the consistency factor an is based on the water to binder ratio and is defined as follows:

$$\gamma_{c,s} = 0,82 + 0,00264s \tag{60}$$

$$\gamma_{sh,s} = 0,89 + 0,00161s \tag{61}$$

Here s is the slump in mm. Cement factors for shrinkage is expressed as follows:

$$\gamma_{sh,c} = 0,75 + 0,00061c \tag{62}$$

Were c is the cement content in kg/m^3. The aggregate factors $\gamma_{c,\psi}$ and $\gamma_{sh,\psi}$ take into account the influence of the content of fines in the mixdesign, and is expressed as follows:

$$\gamma_{c,\psi} = 0{,}88 + 0{,}0024\psi \tag{63}$$

$$\gamma_{sh,\psi} = \begin{cases} 0{,}3 + 0{,}014\psi, & \psi \leq 50\% \\ 0{,}9 + 0{,}002\psi, & \psi > 50\% \end{cases} \tag{64}$$

Here ψ is the percentage of fines, and can be expressed as follows:

$$\psi = \frac{m_f}{m_{agg}} \tag{65}$$

Where m_f is the mass of fines and m_{agg} is the mass of the aggregates. The effects of diffrent aggregates can be seen in Figure 25. Finally there are factors for the Air-content of the concrete, and they are defined as shown below:

$$\gamma_{sh,\alpha} = 0{,}46 + 0{,}09\alpha \geq 1{,}0 \tag{66}$$

$$\gamma_{sh,\alpha} = 0{,}95 + 0{,}008\alpha \geq 1{,}0 \tag{67}$$

Here α is the air content in percentages [53]. To calculate the creep or shrinkage for a specific time then the following equations can be used to estimate it:

$$v_t = \frac{t^{0,6}}{10 + t^{0,6}} v_c \tag{68}$$

$$(\epsilon_{sh})_t = \frac{t}{35 + t}(\epsilon_{sh})_u \tag{69}$$

Here t is the age of the sample after initial curing, f and α are constant and differ with size and shape. The f is in the range of 20 to 130 days and α is in the range of 0,9 to 1,1[53].

2.6.3 The Creep and shrinkage models of Model B3

The third model to be analyzed is the one proposed by Bazant (Model B3) [54, 1]. The model is simple but is supposed to agree better with the experimental data and validate the theoretical than previously used models; The model takes into account more factors than previous models does and is more complex than design code models. It has a different structure than the other were it enables the calculations of separate compliance functions for the basic creep and drying creep. The Model B3 uses the following factors to predicted concrete creep; aggregate to cement ratio, cement content (c), cement type, water to cement ratio, water content, age at loading, age of sample, applied stress (σ), cross-section shape, curing conditions, compressive strength at 28 days, duration of loading, effective thickness (D), elastic modulus at loading (E), elastic modulus at 28 days (E), relative humidity (h), temperature (T) and time of drying commences (t_0). To predict the total strain the following compliance function can be applied:

$$\varepsilon(t) = J(t,t')\sigma + \varepsilon_{sh}(t) + \alpha\Delta T(t) \tag{70}$$

Here $\varepsilon_{sh}(t)$ is the shrinkage strain over time and $\Delta T(t)$ is the change in temperature over time. The applied stress σ is multiplied by:

$$J(t,t') = q_1 + C_0(t,t') + C_d(t,t',t_0) \tag{71}$$

Where q_1 is the instantaneous strain due to unit stress, $C_0(t,t')$ is the compliance function for basic creep and $C_d(t,t',t_0)$ is the function for drying creep.

The instantaneous strain can be taken as $q_1 = 1/E_0$, where E_0 is not the real elastic modulus but more as an empirical modulus. The basic creep compliance is defined by it´s time rate which is defined as follows:

$$\dot{C}_0(t,t') = \frac{n(q_2 t^{-m} + q_3)}{(t-t') + (t-t')^{1-n}} + \frac{q_4}{t}, m = 0,5, n = 0.1 \tag{72}$$

Where $\dot{C}_0(t,t') = \delta C_0(t,t')/\delta t$ and q_2, q_3 and q_4 are empirical factors. By integrating the compliance function above the following is obtained:

$$C_0(t,t') = q_2 Q(t,t') + q_3 ln(1 + (t-t')^n) + q_4 \, ln\left(\frac{t}{t'}\right) \tag{73}$$

Where $Q(t,t')$ is a binominal integral which can´t be by expressed analytically, it can be found by numerical integration. For creep due to drying the following compliance function is applied:

$$C_d(t,t',t_0) = q_5\left[e^{-8H(t)} - e^{-8H(t')}\right]^{0,5} \tag{74}$$

Where q_5 is an empirical factor and $H(t)$ is function based on drying conditions and is further defined in [54] ,as are the empirical factors q_1, q_2, q_2, q_4 and q_5 [28].

3. Phase 1: Long-term research on creep and shrinkages

Most of the research has been started by other researchers and is ongoing; this will be utilized as part of the work and has been continued by the author. The creep and shrinkage data will be presented and used to evaluate the effects of the porous basalt aggregate type (normally used in Iceland) on the volumetric behavior. The methods used to evaluate creep and shrinkage are according to the methods proposed by American Society of Testing and Materials (ASTM).

3.1 Research specimen

Research on the long term effects of concrete creep has been performed at the institute (ICI Rheocenter) for over 10 years. The first samples were cast and put into the creep rigs in 2001, were creep and shrinkage was observed for 1 year. These samples were made with concrete C25, C35 and C50 for three different types of aggregate. The three different aggregates were from different quarries with different porosity (Quarries 1, 2, and 3). The same filler was used for all samples, that being material from quarry 1. After 1 year of testing, new samples were cast and put in the testing rigs, these samples have been observed until this day. These samples were cast using C40, C60 and C70 concrete and same type of aggregates and fillers were used. In the year 2004 samples were cast and put into new creep rigs. These samples are still being observed. They were designed to test what effects a difference in volume percentage of cement paste has on concrete creep. Both conventional vibrated concrete (CVC) and self compacting concrete (SCC) are being tested in two separate rigs. The latest part of the research started in

Figure 28: The two newest creep rigs at the institute

2009 and 2010. These are two rigs, in the rig from 2009 are samples cast from normal concrete (C25) for 3 different types of aggregates. The aggregates are from two quarries in Iceland (Quarry 1 and 2) along with material from Norway (Quarry 4). The samples in the last rig from 2010 are samples of SCC. There are three types of SCC: they are normal SCC with air, ECO SCC without air and ECO SCC with air. The samples in all the rigs are still being tested and will be tested for some years to come.

3.2 Test methods

The methods used to test the creep and shrinkage are described by the American Society for Testing and materials (ASTM). There are two different standards ASTM C512 for testing of creep and the ASTM C157 for shrinkage.

The testing standard for concrete creep measurements

The testing standard ASTM C512 [55] describes the method on how to measure and test creep of concrete in compression. The test method describes a load-induced time-depended compressive strain measured over time under controlled environment. The test method is presented as a method to compare different types of concrete. Creep is proportional to stress up to 40% of concrete ultimate compressive strength and should be measured in that range for comparison of concrete types. Creep is also directly proportional to the cement paste volume in concrete.

Figure 29: Setup for the loading rigs for concrete creep testing[55]

The loading frame used shall be capable of applying and maintain the load. A simple version of the apparatus the standard describes it as consisting of a header plates bearing on ends of the added specimens with a load-maintaining element that can by a spring, a hydraulic capsule or a ram. In each loading frame several specimen can be loaded at the same time. An example of such a loading-frame is presented in Figure 29. The specimen size is 150±1,6 mm and the length shall be at least 292 mm. For the testing there should be cast at least 6 specimen from a given batch of concrete. Two tested for compressive strength, two for creep and two for shrinkage. Creep and shrinkage are measured simultaneously for deformations under the same environmental conditions. Normal curing for specimens in the creep test is after removal from molds at age of 20-48 hours they are placed in 23,0 ± 1,7°C under moist condition (~100%RH). At the age of 7 days the specimen are stored at 23,0 ± 1,1°C and a relative humidity of 50 ± 4% until testing. The specimens are normally loaded at 28 days of age but can also be loaded at 2, 7 or 90 days, or 1 year. The loading shall not exceed 40% of the compression strength of the concrete at the age of loading. Strain measurements are taken before and immediately after loading, 2 to 6 hours after loading and then daily for a week and then weekly for a month and monthly for a year. Before each reading the load is measured and if there is a variation of more than 2% the loading shall be adjusted to the correct value.

Testing standard for concrete shrinkage

This testing standard ASTM C157-99 [56] describes a way to estimate the potential of volumetric expansion or contraction of mortars and concrete. Test samples are cast with a square cross-section that depends on the aggregate size, e.g. for a maximum size of 25mm, a 75×75mm cross-section is used. For a specimen size of 75×75mm cross-section the gauge length of the specimen is defined as 250mm. These are the dimensions used in testing concrete specimen and guidelines for mortar and other aggregate size can be found in the standard itself. After casting,
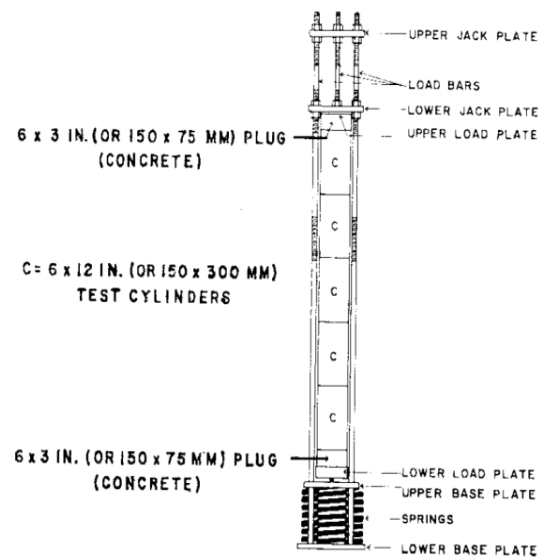
the samples are allowed to rest to the age of 23½ hours and are to be demolded at that time. After demolding the samples are put into lime water for a period of time, which is 30 min for a cross-section size of 75×75mm. The first measurement is taken after 24 +/- ½ hours after adding the water to the mix. There are two different types of curing considered, the sample can be stored in lime water for 28 days or using so called air curing, then the sample is stored at 23°C with 50% relative humidity. The readings are then taken at specific times: 4, 7, 14, 28 days & 8, 16, 32, 64 weeks after curing.

3.3 Materials and design of mixtures

The aggregate used in all specimen came from 4 quarries and in all mixtures blend silica fume cement was used, graded CEM II A-M 42,5R, except for the SCC and EcoSCC, where a cement graded CEM I 52,5N was used. In all mixtures a high-rang water reducer (HRWR) and air-entraining agents were used. As the objective is to evaluate the relation of the high porosity (in Icelandic porous basalt aggregates) and the creep and shrinkage behavior of concrete, four types of coarse aggregates were chosen from different quarries in Iceland and Norway. For quarry 1, the material is taken from the seabed of Kollafjordur. Quarry 2 is in a hill side near Reykjavik, and quarry 3 is a blasted mountain side. These aggregates have 5% to 17% porosity, which is high for conventional aggregate typically used in concrete. The forth type of aggregate is granite material imported from Norway. The main characteristics of the selected aggregate are given in Table 2. The porosity of the aggregates reported in the Table which is estimated using equation 39 on page 39.

Table 2: Characteristics of aggregate from Iceland and Norway

Quarry	Rock type	Size [mm]	Density [kg/m^3]	Water absorption	Porosity
1	Basalt	0-8	2610	4,80%	12,0%
1	Basalt	8-16	2820	2,60%	7,1%
2	Basalt	8-19	2530	7,20%	17,0%
3	Basalt	8-12	2930	2,30%	6,6%
3	Basalt	12-16	2960	1,70%	4,9%
4	Granit	0-8	2650	0,64%	1,7%
4	Granit	8-16	2660	0,70%	1,8%

Mixtures for concrete C40, C60 and C70

The batches for the concrete C40, C60 and C70 were created and cast in 2002, the aim was to determine the effects of different types of basalt aggregate on the creep behavior of concrete. In Table 3 the main values for the batches are presented such as w/c ratio, air and cement content, also the cement paste volume (including air volume), slump and density of the fresh concrete. The variables for these batches were type of aggregate and difference in strength classes and therefore w/c- ratio, but the cement paste volume was constant.

Table 3: The main mixdesign values for C40, C60, C70 and measured values for air, slump and density

	Aggregate Quarry	w/c	Aggregate <4mm [%]	Aggregate <8mm [%]	Air [%]	Cement [kg/m3]	C. Past [%]	slump [mm]	Density [kg/m3]
C40	1	0,37	45	77	7,1	444	38,4	210	2272
	2	0,37	46	58	8,0	440	37,9	130	2228
	3	0,37	45	60	6,0	450	37,6	190	2372
C60	1	0,31	49	75	4,7	505	37,2	80	2409
	2	0,31	47	58	6,2	498	38,2	100	2272
	3	0,31	45	60	4,7	506	37,1	90	2443
C70	1	0,29	48	78	4,0	540	37,6	60	2473
	2	0,29	47	58	6,6	526	39,2	170	2309
	3	0,29	47	60	3,8	540	37,6	160	2517

A significant difference in elastic modulus of the concrete samples can be observed when using the porous basaltic aggregates. It can also be observed that the elastic modulus was the lowest in concrete made with aggregates from quarry 2 (porosity 13.4-14.9%), see Table 4. The measured elastic moduli of all tested mixtures were lower than the calculated values. The spread can be correlated to the degree of porosity of the aggregate, as can be seen in Figure 30. The increase in aggregate porosity from 0% to 40% in concrete made with recycled aggregate is reported to lead to 60% reduction in elastic modulus [19]. It can also be observed that the 28-day compressive strength development of mixtures prepared for different quarries in Iceland are similar, except for the HPC 70 mixture made with aggregates from quarry 2 where lower strength was obtained, see Table 4.

Table 4: Compressive strength and elastic-modulus of tested concrete mixture at 28 days

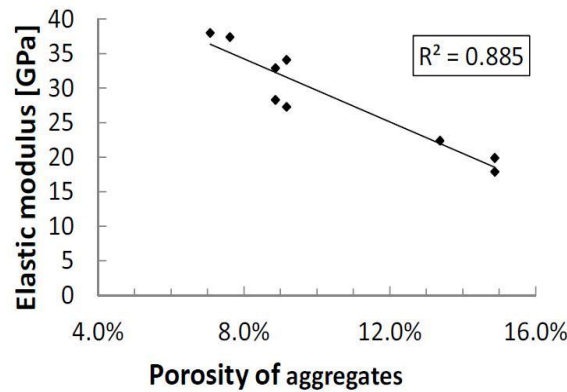|	Aggregate	f_c	E_m	E_{cm}	Diff %
C40	Quarry 1	45,3	27,3	34,6	-21,1%
	Quarry 2	-	17,9	34,6	-48,2%
	Quarry 3	48,2	28,3	35,3	-19,7%
C60	Quarry 1	61,9	34,1	38,0	-10,3%
	Quarry 2	62,8	19,9	38,2	-47,9%
	Quarry 3	62,3	32,9	38,1	-13,6%
C70	Quarry 1	68,2	37,4	39,1	-4,4%
	Quarry 2	62,1	22,4	38,0	-41,1%
	Quarry 3	70,0	38,0	39,4	-3,7%

Figure 30: Variation in elastic modulus of concrete with porosity of aggregate for C40, C60 and C70 mixtures

Mixdesign for concrete CVC and SCC

The batches for the concrete CVC and SCC were created and cast in 2004, the aim was to determine the effects of different values of cement paste volume on the creep behavior of normal and self compacting concrete. In Table 5 the main values for the batches are presented such as w/c ratio, air and cement content, also the cement paste volume (excluding air volume), slump and density of the fresh concrete. The variation between batches here is the cement paste volume and the type of aggregate for both conventional vibrated and self compacting concrete.

Table 5: The main mixdesign values for CVC and SCC, and measured values for air, slump and density

	Aggregate Quarry	w/c	Aggregate <4mm [%]	Aggregate <8mm [%]	Air [%]	Cement [kg/m3]	C. Past [%]	slump [mm]	Density [kg/m3]
CVC 1	4	0,38	47	55	8,4	435	31,1	190	2232
CVC 2	4	0,384	47	55	5,3	360	25,7	140	2326
CVC 3	1	0,394	50	77	3,5	366	26,4	30	2426
SCC 1	4	0,36	54	72	5	450	36,7	n/a	2361
SCC 2	1	0,39	54	72	4,5	394	34	n/a	2300
SCC 3	4	0,37	49	77	6	450	37	n/a	2288

Mixdesign for C25 mixtures

The batches for the concrete C25 were created and cast in 2009, the aim was to determine the effects of different types of aggregate, from Iceland and Norway. In Table 6 the main values for the batches are presented such as w/c ratio, air and cement content, also the cement paste volume (including air volume), slump and density of the fresh concrete. The variation between batches is the aggregate, the type and the amount of porosity. The aggregate type is basalt and granite aggregate, and they vary in porosity from about 1,5% to around 17,0%.

Table 6: The main mixdesign values for concrete C25 with different types of aggregate

	Aggregate Quarry	w/c	Aggregate <4mm [%]	Aggregate <8mm [%]	Air [%]	Cement [kg/m3]	C. Past [%]	slump [mm]	Density [kg/m3]
	1	0,55	47	58	5,6	316	33,4	110	2350
C25	2	0,55	45	66	5,5	315	31,9	130	2296
	4	0,55	45	52	4,9	320	33	150	2300

Mixdesign for Eco-SCC mixtures

The batches for the self compacting concrete and Eco self compacting concrete were created and cast in 2009, the aim was to determine the effects of different types of self compacting concrete. In Table 7 the main values for the batches are presented such as w/c ratio, air and cement content, also the cement paste volume (including air volume), slump and density of the fresh concrete. The main variations between batches is the type of SCC, they are SCC including an air entrapment agent (AEA), SCC with lower cement content than normal with and without AEA. Due to the lower amount of cement content the SCC is considered environmentally friendly, because of the lower amount of CO_2 emissions per cubic meter of concrete. This type of SCC is called EcoSCC.

Table 7: The main mixdesign values for SCC with air entrainment, EcoSCC with and without air entrainment

	Aggregate Quarry	w/c	Aggregate <4mm [%]	Aggregate <8mm [%]	Air [%]	Cement [kg/m3]	C. Past [%]	slump [mm]	Density [kg/m3]
SCC AEA	4	0,34	58	73	7,2	549	45,3	270	2184
EcoSCC	4	0,61	60	79	1,3	316	30,8	270	2343
EcoSCC/AEA	4	0,58	60	79	5,7	316	34,4	270	2246

3.4 Results

In this chapter there will be a presentation of the results for the creep and shrinkage research conducted for more than a decade at the Innovation Center Iceland. The experimental concrete mixtures are divided into chapters, the oldest research first.

C40, C60 and C70 mixes

Creep strains for the C40 mixture prepared using different types of aggregate are shown in Figure 31. The lowest creep measurements corresponds to the material with the lowest modulus of elasticity, which is that made with aggregate from Quarry 2 (porosity 13,4%-14,9%). However, the difference in creep behavior is limited to 0.1 mm/m. In the case of the C40 mixture, the creep results were similar for all mixtures made with basalt aggregate obtained from the various quarries from Iceland. On the other hand, in the case of the C60 and C70 mixtures, those made with aggregate form quarry 2 had considerably greater creep than those containing aggregates from quarries 1 or 3 (porosity 7,1%-9,2%). This can be related to the stiffness of the coarse aggregate since aggregate from quarry 2 had considerably greater porosity (17%) compared to those of quarry 1 and 3 (7,1% and 6,6%). Higher porosity leads to lower elastic modulus (Figure 1), thus reducing the ability of the aggregate to restrain deformation in the

concrete, resulting from the sustained loading. This phenomenon was not observed in the case of the C40 mixture since the paste itself was porous. On the other hand, in the lower porosity mixtures, the effect of aggregate porosity, and hence its effect on creep, are more apparent.
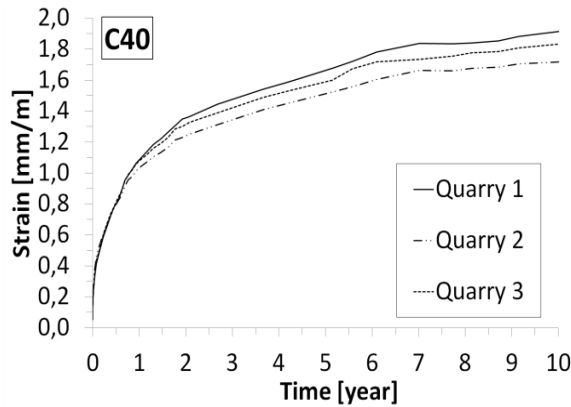

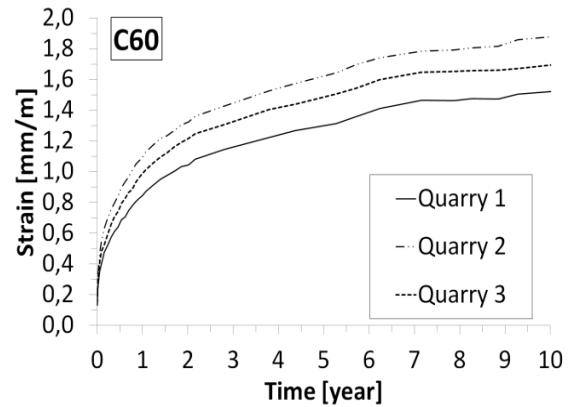**Figure 31: Creep development over 10 years for C40 concrete using various aggregates**

Figure 32: Creep development over 10 years for C60 concrete using various aggregates
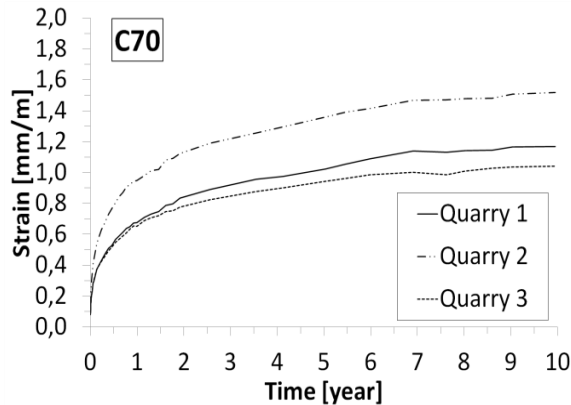

Figure 33: Creep development over 10 years for C70 concrete using various aggregates

Figure 34 shows the specific creep for the tested mixtures prepared with aggregate from quarry 1. The specific creep is calculated as the creep strain divided by the applied load, which is about 33% to 36% of 28 day compressive strength. The specific creep of the specimens seems to be progressing normally, though it still appears to be increasing even after 10 years. The difference in specific creep between strength classes is logical because of the difference in compressive strength and in elastic modulus. From Figures 35 and 36 the specific creep for concrete made with aggregate from quarries 2 and 3 is presented. Similarly, the specific creep increases with lower strength classes. The variation is that the specific creep seems to differ less as the porosity of the aggregate increases. This could be due to the fact that there is less difference between the elastic modulus of the different strength classes, when using the aggregate from quarry 2 which has the lowest porosity.
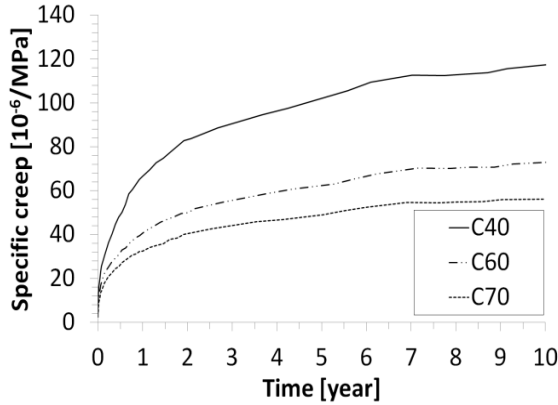
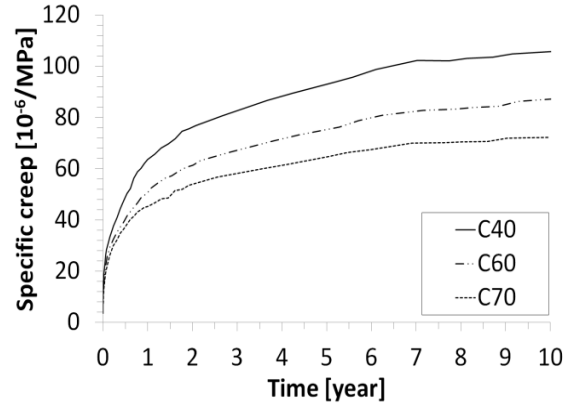**Figure 34: The specific creep for concretes cast with aggregates from quarry 1 (porosity 7.6-9.2%).**

Figure 35: The specific creep for concretes cast with aggregates from quarry 2 (porosity 13.4-14.9%).
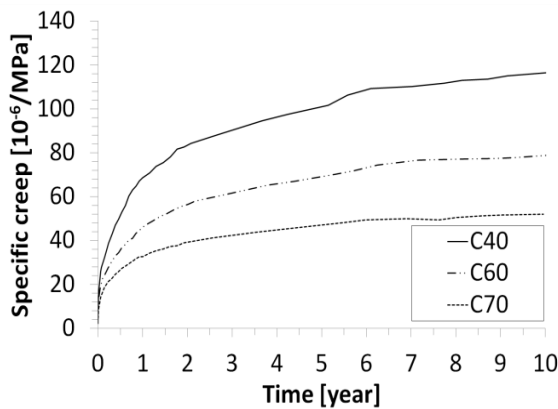

Figure 36: The specific creep for concretes cast with aggregates from quarry 3 (7.1-8.9%).

CVC and SCC mixes

The creep development for the conventional vibrated concrete (CVC) can be observed in Figure 39, where CVC 1 is the concrete mixture made from granite with the highest cement paste volume. The standards say that with increased paste volume the creep increases and this can be observed in the figure, as the mixture CVC 2 is of same composition with lower paste volume. In the mixture CVC 3 Icelandic basalt aggregate is used as an alternative to the Norwegian granite aggregate. It can be observed that the mixture CVC 3 experiences less creep than CVC 2, which has about the same paste volume. This is not normally the case when observing the creep behavior using porous Icelandic basalt as aggregate.

In Figure 38 the creep growth of self compacting concrete (SCC) is shown, where the main difference is in paste volume and the type of aggregate. The mixtures have different cement paste volume with SCC 1 and SCC 3 containing the Norwegian Granite aggregate which has paste volume of 37% compared to 34% in SCC 2 prepared with basalt aggregate from Quarry 1. Again, despite of the lower paste volume (quarter aggregate volume) SCC 2 made with the porous aggregate gives higher creep, which was approximately 0.2 mm/m after 8 years.
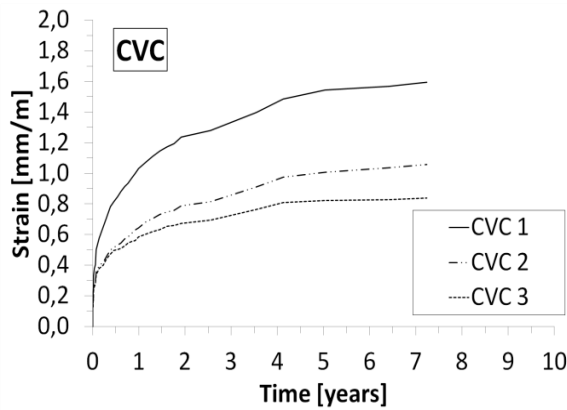
55

Figure 37: The creep development for CVC using aggregates from both Iceland and Norway using different cement paste volumes
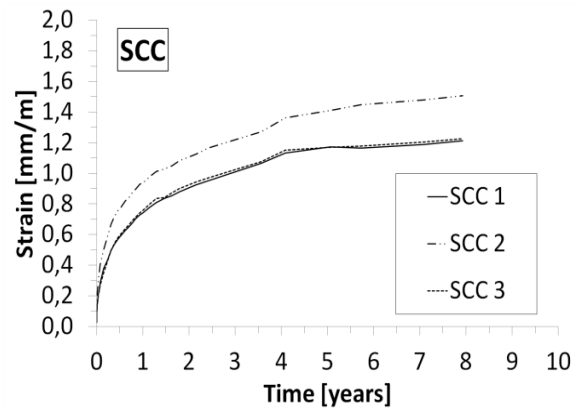
Figure 38: The creep development for SCC using aggregates from both Iceland and Norway using different cement paste volumes

In Figures 39 and 40 the specific creep for the CVC mixtures and SCC mixtures is presented. It can be observed from the pictures that the specific creep is much higher for the CVC with the same cement paste volume. It should be noted that the SCC mixtures have significantly lower specific creep than the CVC.
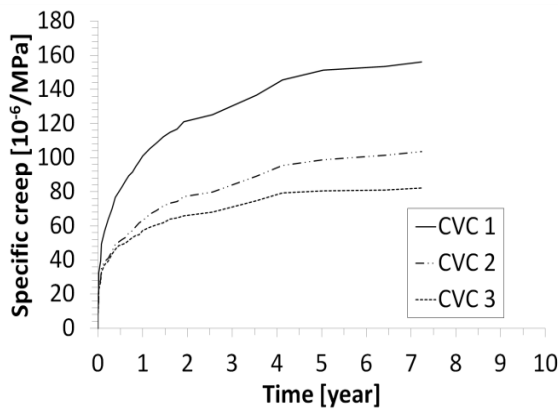
Figure 39: The specific creep development for CVC concrete
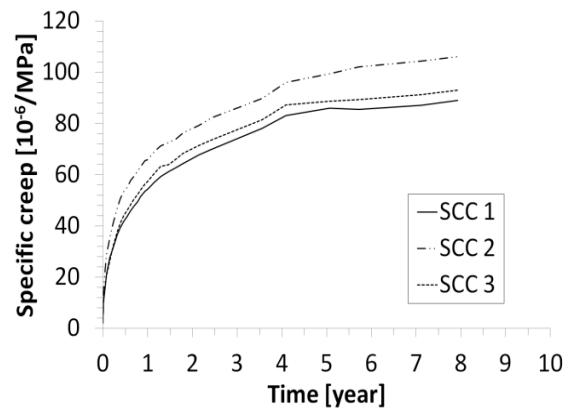
Figure 40: The specific creep development for SCC using aggregates from both Iceland and Norway

C25 mixtures with different types of aggregate

In Figure 41 the creep progress of C25 concrete mixtures using different types of aggregate is presented. It can be seen from the figure that the mixture using aggregate from quarries 1 and 2 are somewhat higher than the mixture using materials from quarry 4. The aggregate in quarries 1 and 2 are porous basalt but the aggregate from quarry 4 is granite with low porosity. It seems that using highly porous basalt aggregate in the mixture increases the creep growth. It is should be noted, although the aggregate from quarry 2 is more porous the creep for the concrete specimen is lower than for specimen using materials from quarry 1.
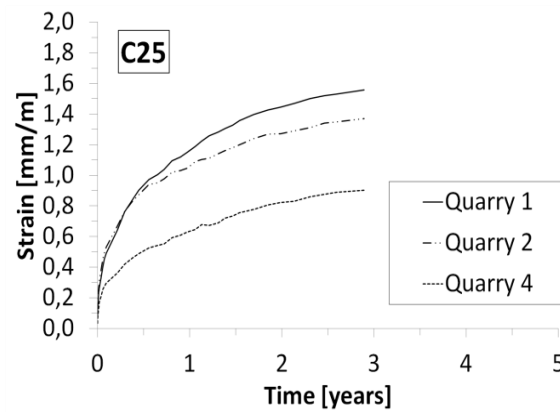
Figure 41: The creep development for C25 using aggregates from three quarries in Iceland

SCC, Eco-SCC AEA and Eco-SCC

Figure 42 shows the creep development of self compacting concrete (SCC) using both low and normal cement amount (Rich SCC, about 450 kg/m³). The mixtures named EcoSCC have low cement content. It can be observed that the mixtures express low creep values compared to what has been observed previously in this chapter. Both mixtures using lower cement content seem to creep more than the normal SCC mixture. From Figure 43, the shrinkage of the samples can be observed and same as for the creep development, the shrinkage is grater for the EcoSCC mixtures. This is not what was to be expected as there is lower cement (and therefore less cement paste) the shrinkage should be less.
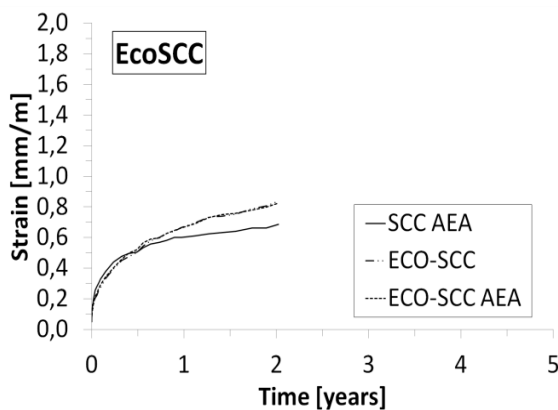
Figure 42: The creep development for SCC and EcoSCC
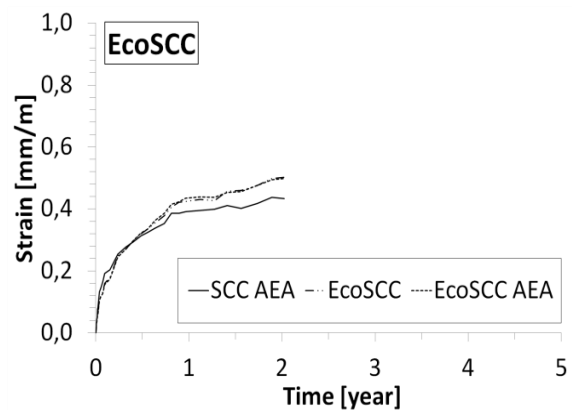
Figure 43: The shrinkage development for SCC and EcoSCC

Modeling calculations and comparison to experimental data

The models defined in chapter 2.6 were used to estimate strains due to creep in concrete specimen. The estimated strains using the measured values for the elastic modulus of the concrete and compressive strength are given in Table 4 and compared to creep measurements. Table 4 compares the measurements of creep deformation to estimated values. Creep is estimated for the C40 concrete cast with aggregate from quarry 1. In Table 4, creep development

57

and estimation are shown for the C70 HPC made with aggregates from quarry 1 (porosity 7.6-9.2%).
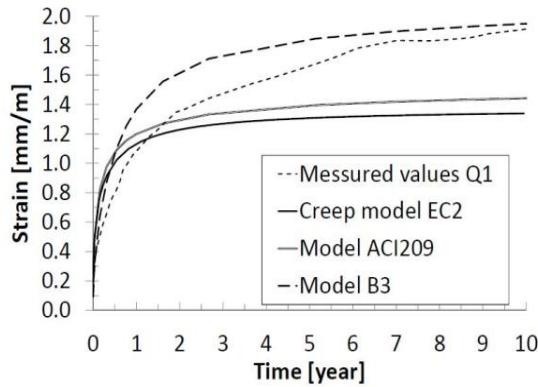
Figure 44: Creep development over 10 years for Normal C40 concrete using aggregates from quarry 1 (porosity 9.2%) and the creep estimation of the models.
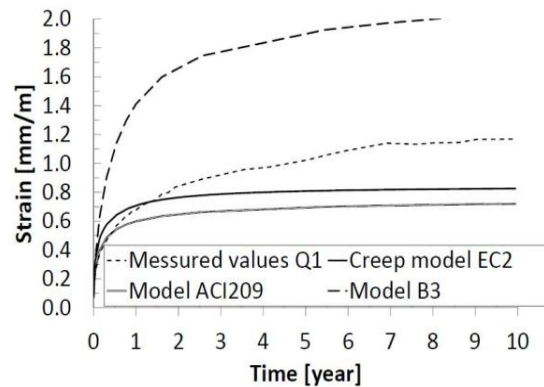
Figure 45: Creep development over 10 years for HPC C70 concrete using aggregates from quarry 1 (porosity 7.6%) and the creep estimation of the models.

From Figures 44 and 45, it is clear that the long-term estimated creep values are lower than the measured values for both the EC2 and ACI209 models. For both cases, the measured creep exceeds predicted values after 1 year. After 10 years of loading, creep was still increasing and exceeded the estimated values by about 40%.

Figure 46 compares the creep data to predicted values from the EC2 model for the C40, C60 and C70 mixtures made with aggregates from different quarries. It can be seen that the model predicts greater creep than the actual data when the creep is limited to 0.6 mm/m. As creep strain increases, the model seems to diverge from actual values. Concrete made with coarse aggregate from quarry 2 experienced less creep than predicted values.
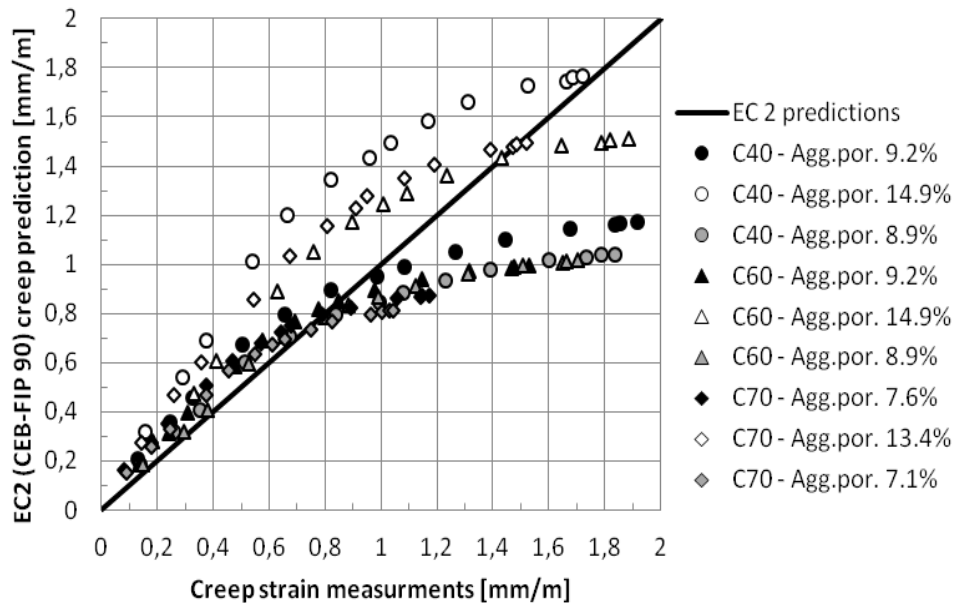
Figure 46 : Creep prediction of the EuroCode 2 creep model compared to measured values
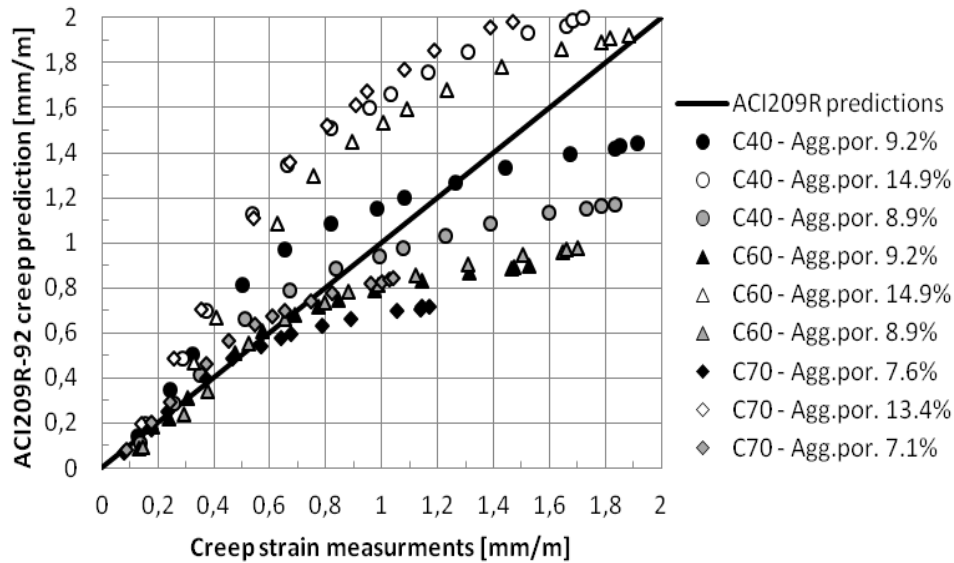
Figure 47 : Creep prediction of the American Concrete Institute creep model compared to measured values
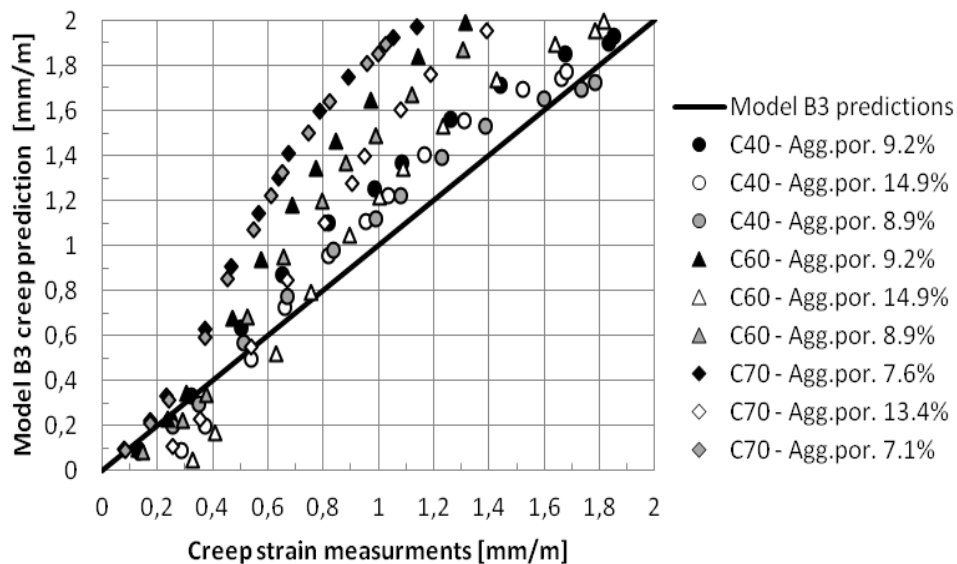
Figure 48 : Creep prediction of the B3 creep model compared to measured values

In Figure 47 a comparison of measured values to calculated values is presented for the ACI209 model. The measured values are mostly diverging from the calculated values of studies beyond 0.8 mm/m. There is an exception for the calculated concrete made with aggregate from quarry 2. This is due to the high porosity and low elastic modulus of the aggregate.

In Figure 48, comparison of measured values to calculated ones according to the B3 model is given. The B3 model overestimates creep, especially the long-term values which correspond to high creep values. The model seems to overestimate the specimen in higher strength classes, regardless of the aggregate. Characteristics and connected strength class, the long-term B3 model creep values, can be approximately 10% to 75% higher than predicted values.

Shrinkage of samples and comparison to models

In this section results will be presented for shrinkage samples that were tested simultaneously as the creep mixtures also presented in this chapter. The specimen presented are of three types of concrete using four types of aggregate with the aim of seeing how the porosity of aggregate affects the shrinkage of concrete. In Figure 49 the results for shrinkage samples can be observed, where strength class C25 was used. It can be observed from the figure that as the porosity of the aggregate increases the shrinkage increases as well. However, it can be noted that the aggregate with porosity of 1,2% is granite aggregate and seems to have very similar shrinkage behavior as the basalt aggregate with a porosity of 9,1%. In this figure there is also a estimate calculated using EC2 and ACI209 and it can be observed that EC2 overestimates the shrinkage at first but as time passes the shrinkage converses with the EC2 estimate. This is valid for both of the samples with lower aggregate porosities but for the one with higher porosity the estimate is nearly half of the shrinkage. As for the estimate for the ACI209 the estimate is higher than the EC2 estimate.

In Figure 50, the shrinkage for concrete strength class C40 is presented and it can be observed that porosity of the aggregate seem to increase the shrinkage of the samples. The concrete samples with porosity of around 9% report similar shrinkage strains and the samples with about 50% higher porosity has nearly 1/3 higher shrinkage. As before the EC2 underestimates the final shrinkage but overestimates the early shrinkage. The same can be said about the ACI209, it overestimates the early shrinkage but it also overestimates the finale shrinkage.

In Figure 51, measured shrinkage for concrete of strength class C60 is presented. The same as for concrete strength class C40 the shrinkage seems to increase with increased porosity. And as before EC2 underestimates the final shrinkage and ACI209 overestimates the final shrinkage. Figure 52 shows the shrinkage as a function of porosity of the aggregate. It shows that as the porosity of the aggregate increases the shrinkage seem to increases as well.

Figure 49: Shrinkage over 3 years of concrete (strength class C25) made with aggregates with variations in porosity. Also reported are the estimated values for both EC2 and ACI209.

Figure 50: Shrinkage over 3 years of concrete (strength class C40) made with aggregates with variations in porosity. Also reported are the estimated values for both EC2 and ACI209.
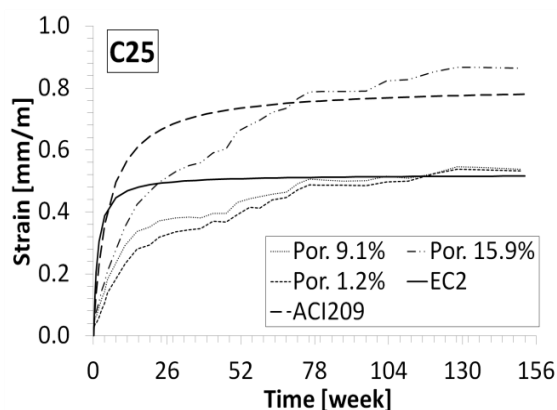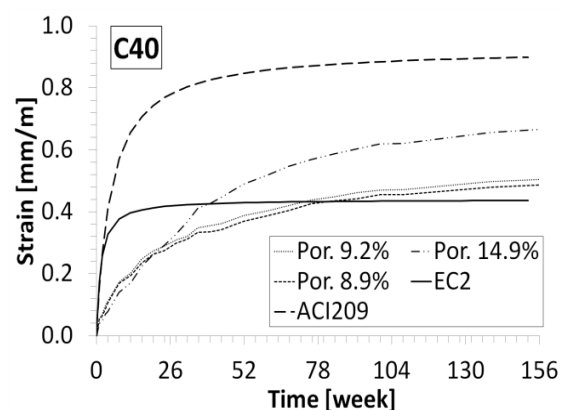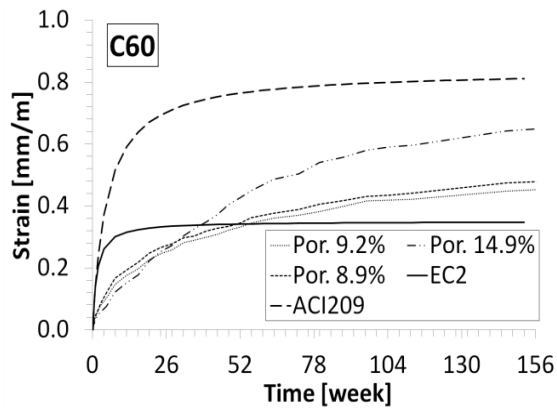
60

Figure 51: Shrinkage over 3 years of concrete (strength class C60) made with aggregates with variations in porosity. Also reported are the estimated values for both EC2 and ACI209.
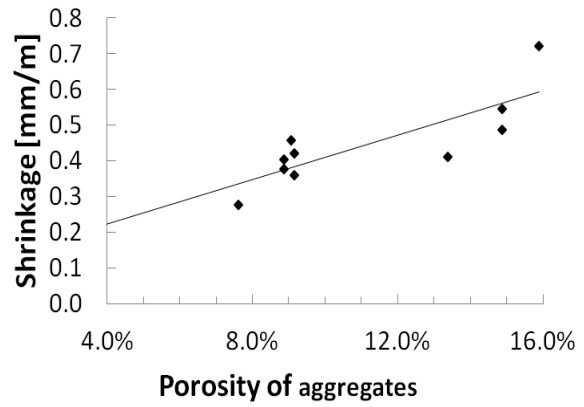

Figure 52: Shrinkage verses the porosity of the aggregate at 64 weeks for aggregates presented in Table 2.

4. Phase 2: Elastic modulus of concrete composites and porous aggregate

In this phase of the experiment the elastic modulus of the concrete and the materials of the concrete composite is measured and analyzed. Materials from Iceland will be tested using standard test methods as well as using new technology. Firstly, rock material from two quarries will be tested for mechanical properties, where the main interest is in the elastic modulus of the materials as they are used as aggregate in large part by Icelandic concrete producers. The elastic modulus of concrete has been measured low for the concrete using these aggregate and this is related to elastic modulus of the aggregate. The concern is that the elastic modulus of the aggregate lowers as the water absorption of the aggregate increases. Secondly, the concrete using aggregate from these two quarries will be used and the concrete specimen tested for mechanical properties. Finally, these will be analyzed together with the mechanical properties of the rock material and the relations presented.

4.1   Test methods

Intact rock cores

Test methods for testing the mechanical properties of rock materials are derived from EN1097-6[57], where test methods for aggregate are presented. The test methods describe how to measure the density and water absorption of the aggregate and from this the porosity can be calculated. These methods are normally used when testing aggregate used in concrete, consequently they give a good representative for comparison. The intact rock samples are treated as large aggregate and using a so called wire basket method the density and water absorption is measured. The weight of the sample is measured under water (at temperature of $22 \pm 3°C$) in the wire basket after the sample as been submerged in water (at temperature of $22 \pm 3°C$) for a period of $24 \pm 0,5$ hours. The sample is then dried in dry cloth and weighed as saturated surface dry. The sample is then put into an oven at $110 \pm 5°C$ to dry completely and get dry weight of the sample. From theses measured weights both the density and water absorption of the sample can be derived.

For the measurements of the mechanical properties of the intact rock specimen the standard ASTM D7012 [58] is used, Method C for the uniaxial compression strength and Method D for the elastic modulus under uniaxial compression load. As described by the standard, the intact rock core specimen shall be drilled and cut into length and the end machined flattened. Then the specimen is placed in a loading frame, if strain gauge (a minimum of two for each direction) are used they should be applied before placement. The loading is then continually applied at rate of 0,5-1,0 MPa (0,8 MPa was used in this case) until failure. At the same time the deformation is logged as a function of loading. From these measurements the elastic modulus, compressive strength and Poisson´s ratio can be derived.

To measure the porosity of the rock cores very accurately, an X-ray Tomography device was utilized. The X-ray Tomography device is of the type nanoCT and is named Phoenix nanotom. It can capture 3D images of samples in the range from small geological specimens to medium size industrial parts. It gives good quality data on the magnitude of voids in the samples

and can also give the particle density of the material; this ability could not be utilized as the core specimens were too dense to measure. To get the best quality imagery a Gaussian filter was applied of an order of 5, which gave the best results of the 3 filters that were tested.

Concrete specimens

A compressometer was used to measure the elastic modulus of concrete, as well as strain gauges. The method is described in ASTM C 469 [59] to determine the tangent elastic modulus (E_m) of cylinders measuring 150 x 300 mm. The strain gauges were of sufficient size and placed accordingly. The load increased steadily up to a preloading of 0,5 MPa and then increased up to a load of 1/3 of the compressive strength of the concrete cores. The load was kept constant for 60 seconds and then unloaded back to the preload, and held there for another 60 seconds. This was then repeated three more times and measurements for deformation taken at preloading and at maximum loading. The measures were then utilized to derive the Elastic modulus for the concrete specimen. Finally, the specimen where all loaded to ultimate compression load.

4.2   Intact rock core Specimens

The specimens to be tested were collected from two quarries in Iceland. For quarry 1, the material is taken from the seabed of Kollafjordur. Quarry 2 is material from a hill side near Reykjavik, same as in chapter 3. To get intact rock specimen large aggregate were collected and core samples were drilled from them. In Figures 53 and 54 the specimens are presented and it can be seen how the porosity varies between samples.

Figure 53: Intact rock specimens from quarry 1
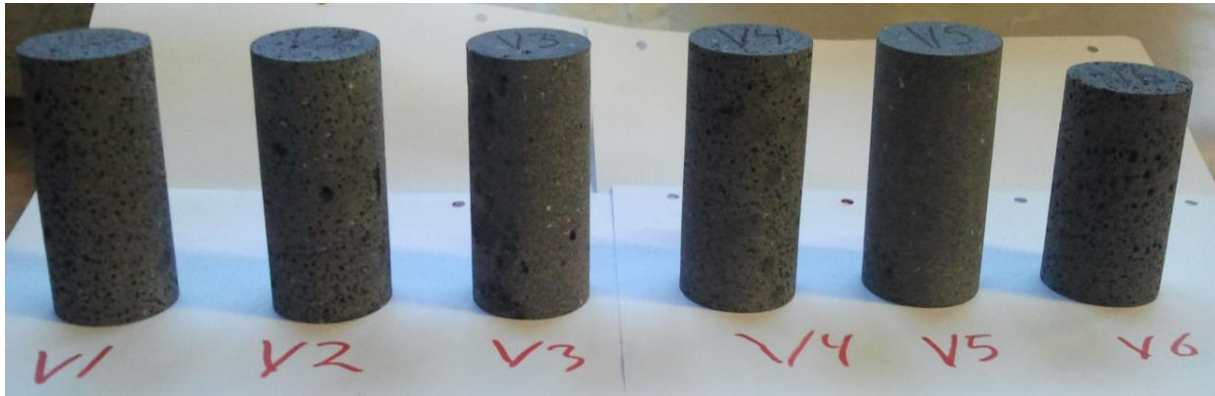
Figure 54: Intact core specimen from Quarry 2

4.3 Experimental results intact rock specimen

The intact core specimens were tested for density and water absorption using commonly used methods for large aggregate. From these basic values from the aggregate cores the porosity can be estimated by using equation 39 to calculate it. The porosity was also measured using x-ray tomography device for comparisons; this will be discussed further later on. The mechanical properties of the core specimen were to be tested to get a comparison between the density and porosity. These core specimens were then tested for elastic modulus, Poisson´s ratio and strength. The results are presented in Table 8.

Table 8: Intact rock core specimen measurement results

		Density [kg/m3]	Water absorption	Calculate Porosity	Porosity x-ray t.	Strength [MPa]	Elastic modulus [GPa]	Poisson's ratio
Quarry 1	B1	2870	1,0%	2,7%	-	299,98	65,9	-
	B2	2742	1,1%	2,9%	1,7%	196,48	64,0	0,26
	B3	2772	1,0%	2,8%	3,0%	139,33	80,8	0,26
	B4	2782	1,2%	3,4%	-	208,34	64,0	-
	B5	2397	2,5%	5,8%	8,2%	96,7	41,5	0,25
	B6	2247	5,1%	11,0%	-	-*	-	-
	B7	2487	5,2%	12,3%	-	45,8	-	-
Quarry 2	V1	2294	1,6%	3,7%	-	83,86	37,8	-
	V2	2393	2,1%	4,9%	7,0%	116,66	48,3	0,14
	V3	2449	1,2%	3,0%	-	190,7	50,6	-
	V4	2374	1,4%	3,3%	7,3%	161,58	50,8	-
	V5	2512	1,2%	3,0%	6,2%	180,36	48,9	0,16
	V6	2361	1,4%	3,3%	-	168,88	39,8	-

*compressive failure before the test load of 30 MPa was reach

X-ray tomography

There were conducted 3D x-ray scans of six specimens, three for each quarry. The specimens were chosen randomly three from each quarry and dried out to prepare for testing. The x-ray scanning device was of type nanoCT. The idea was to 3D scan the specimens to get the porosity of them and the practical density. As mentioned previously, the density could not be estimated as the specimen cores were to big in size verses density of them. The cores could not be lowered in size as the elastic modulus and the strength was to be measured and the cores need to be in sufficient size to be measured. The scanning area was also reduced to about half of the height of the specimen to get quality resolution. All the specimen were then scanned and analyzed one by one, each scan took about 4 hours and the analyze about 2,5 hours. In the scan result analysis, a filter was applied to the specimen, three filters were tested, median filter with 5 iterations and Gaussian filter with both 5 and 7 iterations. The best result was obtained using a Gaussian filter with 5 iterations. To be able to calculate the volume and density of the specimen the grayscale needed to be calibrated, to do that an automatic function in the software was used where the peaks of the grayscale are assumed as the difference between air voids and the most dense material. From that there was a volume analysis and the total volume and the void volume calculated from the grayscale calibration. In Figure 55, the first core is shown were the difference of voids and solid material can be seen and the porosity is presented. The same can be seen in Figure 56 were the voids are more clear as the porosity is more than double. In Figures 57 to 60 the rest of the cores can be observed.
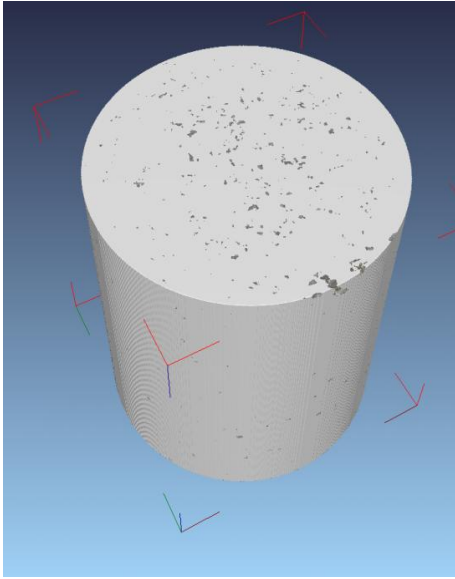
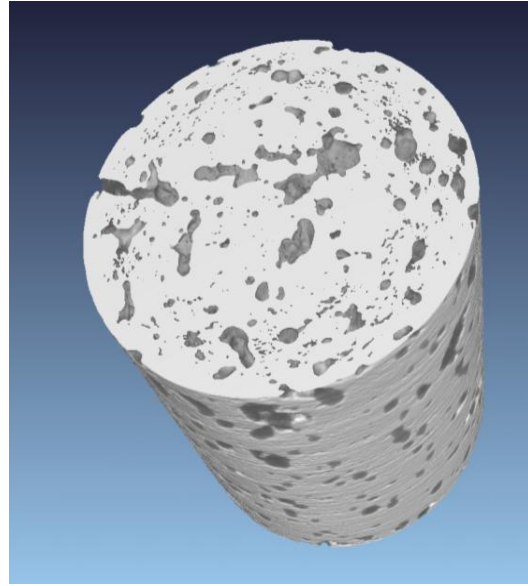**Figure 55: Rock core sample B3, prosity 3,0%**

Figure 56: Rock core sample B5, porosity 8,2%
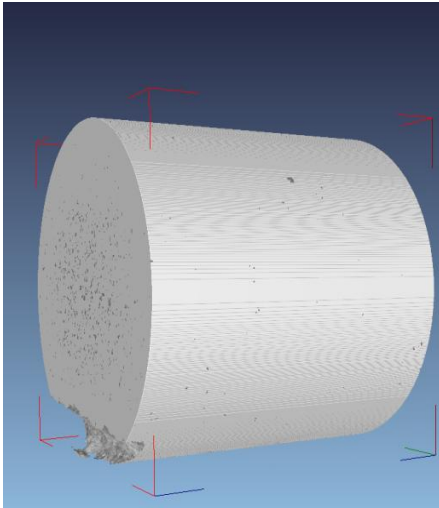
Figure 57: Rock core sample B2, porosity 1,7%
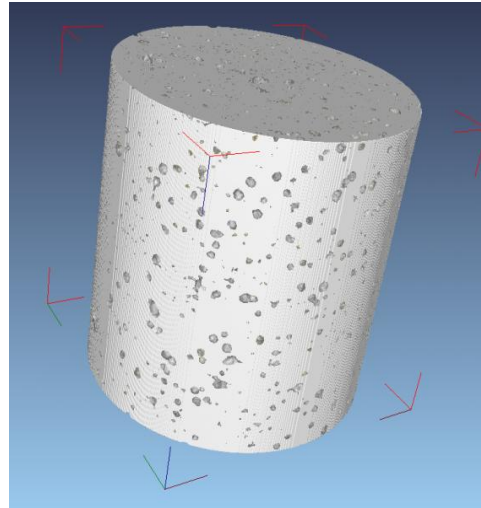
Figure 58 Rock core samples V4, porosity 7,3%
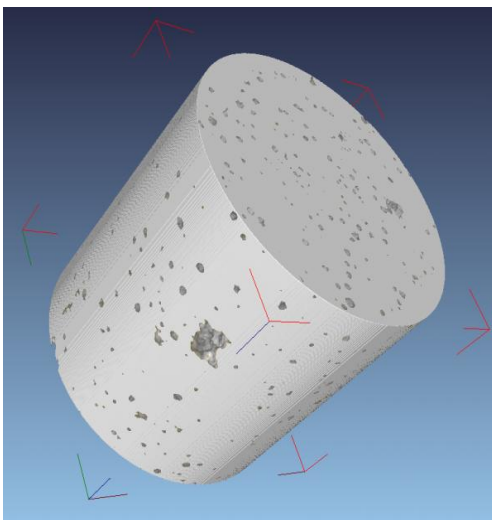
Figure 59: Rock core sample V2, porosity 7,0%
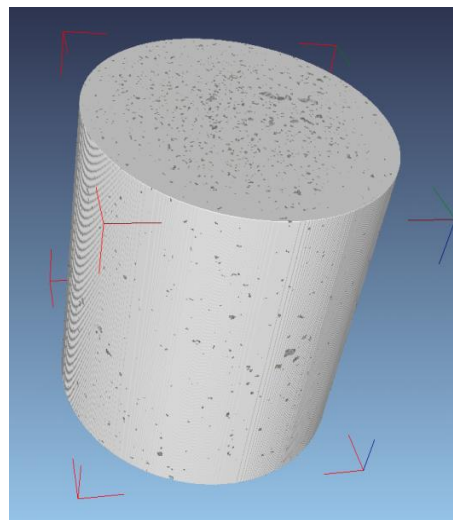
Figure 60: Rock core sample V2, porosity 6,2%

Connections for properties to the increase in porosity

One of the main objectives of the research was to connect the porosity of the aggregate to the decrease in elastic modulus. The measured elastic modulus plotted verses the porosity of the aggregate specimen cores can be seen in Figure 61. There is a correlation between the porosity and the elastic modulus although it is not certain whether it is a linear relation; more research is needed to determine that. It is observed that as the porosity increases from about 3% to nearly 6% the elastic modulus goes down from about 65 GPa to nearly 40 GPa. In Figure 62 the ultimate compressive strength is shown in relation to the porosity. There is a trend that as the porosity goes down the elastic properties go down, but the results are not conclusive and further research needs to be conducted. From the results it is definite that the porosity affects the strength of the specimen by lowering the strength as the porosity increases, but not in a linear manner. With an increase in porosity of about 3% the strength goes down about 50%, same as for the elastic modulus.
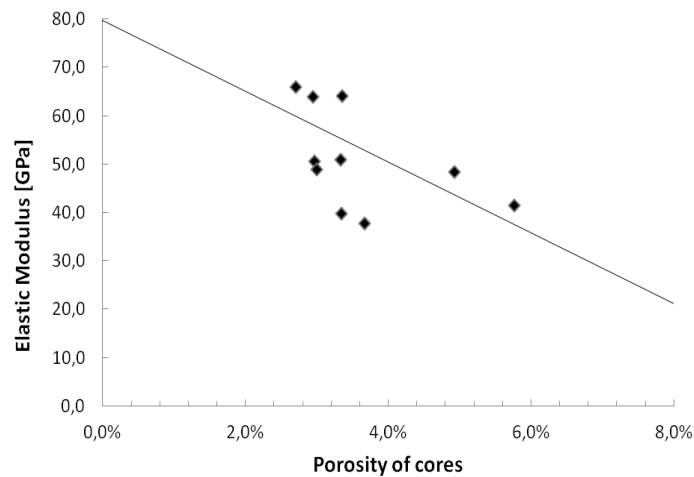
Figure 61: The measured elastic modulus as a function of porosity for the aggregate rock core specimen
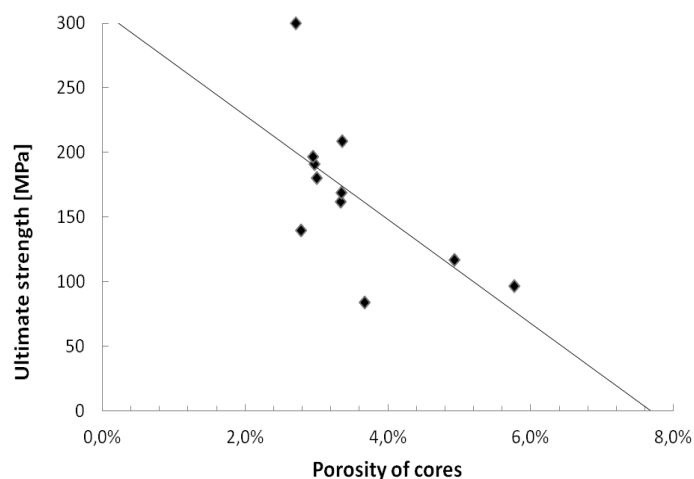
Figure 62: The measured ultimate strength as a function of porosity for the aggregate rock core specimen

Connection of density of materials to mechanical properties

The elastic modulus of a material is often in correlation to its density. The correlation of the rock core specimen density and elastic modulus is high, seen in Figure 63, as could be expected. When the density increases from about 2300 kg/m^3 to 2800 kg/m^3 the elastic modulus increases by about 100%. The correlation between the density and ultimate compression strength is also of interest and is shown in Figure 64. There the correlation is not as good as for the elastic modulus but seems to be linear same as for the elastic modulus.
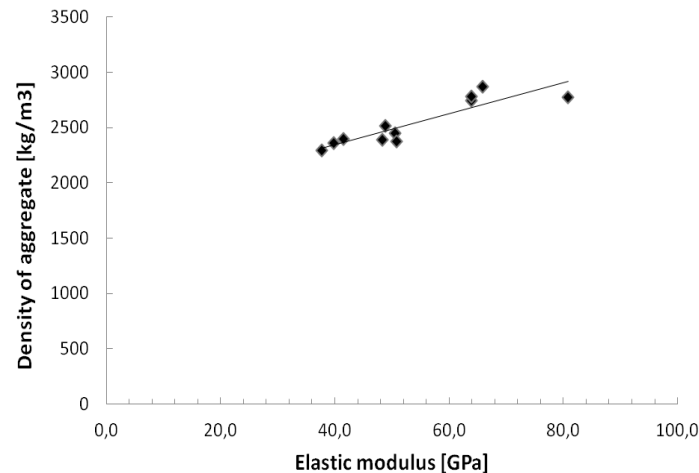
Figure 63: Density of the aggregate as a function of elastic modulus
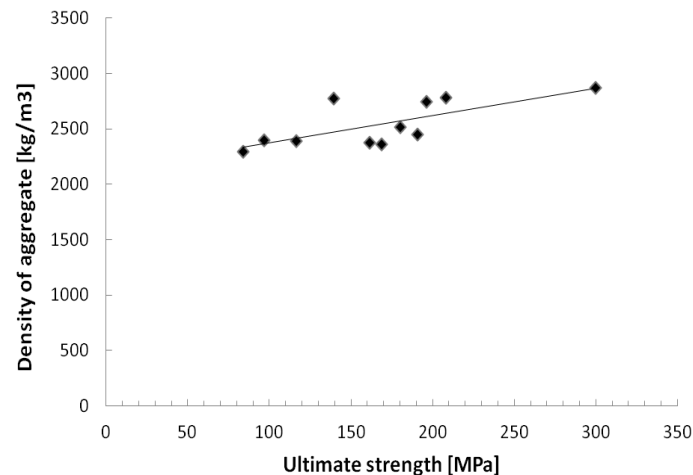
Figure 64:Density of the aggregate as a function of ultimate compression strength

4.4 Experimental results on concrete specimen

A test for the elastic modulus for concrete was performed to be able to compare to the results from the aggregate testing. These were of interest to compare the models in section 0, the models are presented in 2.2.2. Two mixtures were cast to evaluate the elastic modulus of the concrete using aggregate from quarry 2 and w/c ratio of 0,59. Specimens were cast as cylinders 150x300 mm, which is the normally used for testing elastic modulus of concrete using a compressometer. Cube3s were also cast and from those drilled core specimens were created to be tested for elastic modulus using both compressometer and strain gauges.

Strength and elastic modulus results

In Figure 65 the results for the cylinders measuring 150x300 mm are presented. The compressive strength of the specimen is all in the same range of about 30 MPa. The differences in strength can be observed from Figure 65 were the mean strength for mixture 1 is 29,7 MPa and for mixture 2 is 29,6 MPa. In the same figure the elastic moduli of the concrete cylinder specimens is presented, measured using a compressometer. It can be observed that the elastic moduli between specimen varies to some extent. The mean value for the elastic modulus for concrete mixture 1 is 17,9 GPa with a standard deviation of 1,4 GPa and the lowest value is 16,9 GPa. For mixture 2 the mean value is 17,4 GPa with standard deviation 2,3 GPa and a low value of 14,8 GPa. It should be noted that the mixtures have a w/c ratio of 0,59.
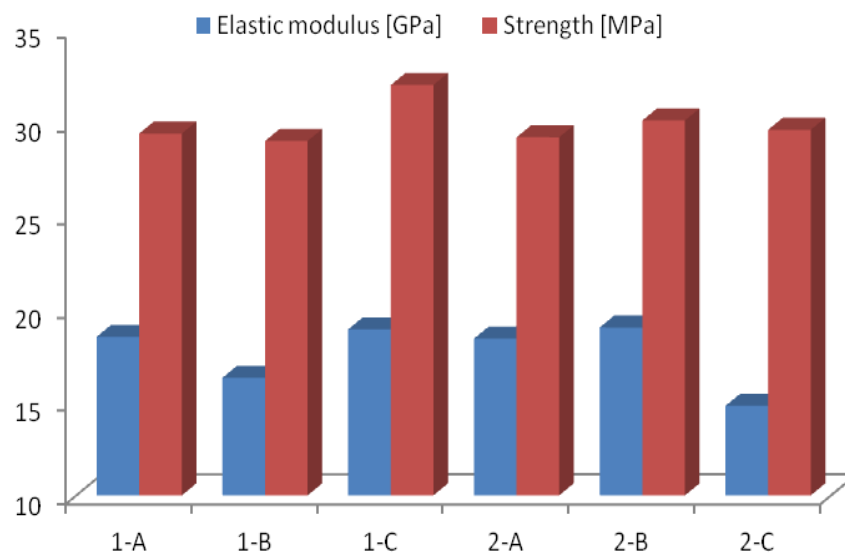
Figure 65: Measured elastic moduli and strength for large cylinders
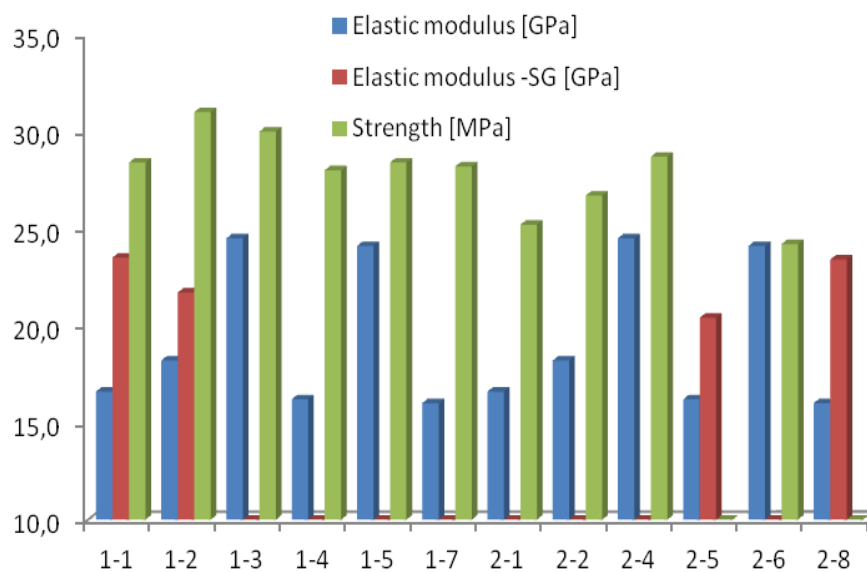
Figure 66: Measured elastic moduli both with and without strain gauges(SG). Strength of the specimen is also presented

The results for the concrete core specimen testing are presented in Figure 66 for both mixture 1 and 2. There is a greater variation in results for the core specimen than there are for the cast cylinder specimen. The strength varies a bit, with a high value of 31 MPa and a low of 28 MPa for mixture 1. For mixture 2 the high value was 28,7 MPa and the low is 24,2 MPa. The elastic moduli of the core specimens for both mixtures vary greatly and there are large differences between values measured with a compressometer and strain gauges, where the strain gauges give much higher values.

Data error for strain gauges

When measuring with strain gauges the concrete core exhibited lower values of strain. This in fact gives higher values for the elastic moduli of the concrete specimen. The hypothesis arose that when strain gauges are placed on more aggregate than cement paste; the value for the elastic modulus would increase as the aggregate exhibit lower strain under the same load (has a higher elastic modulus). So the strain gauges would by increasingly measuring localized elastic modulus rather than the elastic modulus of the core specimen as a whole. So one concrete core was used to test this hypothesis; using four strain gauges placed in on the core with different amount of aggregate to measure the difference in elastic modulus. In Figures 67-70, the four strain gauges are shown (the figures are rotated 90°) portraying how they have different amount of aggregate pacing under the measuring area.

Figure 67: Strain gauge 1 running through 45% aggregate and the elastic modulus estimate from strain was 24,8 GPa
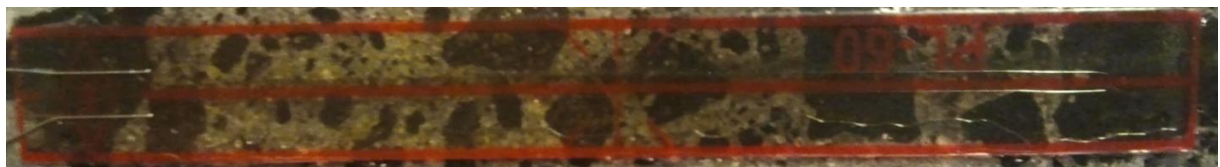
Figure 68: Strain gauge 2 running through 38% aggregate and the elastic modulus estimate from strain was 22,6 GPa

Figure 69: Strain gauge 3 running through 31% aggregate and the elastic modulus estimate from strain was 20,3 GPa

Figure 70: Strain gauge 4 running through 50% aggregate and the elastic modulus estimate from strain was 27,4 GPa

The amount of aggregate the center line passes through, that length divided by the total length of the strain gauge gives the aggregate percentage in Figure 71. From the strain measured the localized elastic modulus is estimated and also given in the figures. The results of the four strain gauges are given in Figure 71 where the elastic modulus is measured locally as a function of the aggregate pass-through. It can be observed that as the aggregate pass-through of the strain gauge increases the localized elastic modulus increases. As the aggregate pass-through increases by about 20% the elastic modulus increases from about 20 GPa to 27 GPa, this can be considered as a large increase.
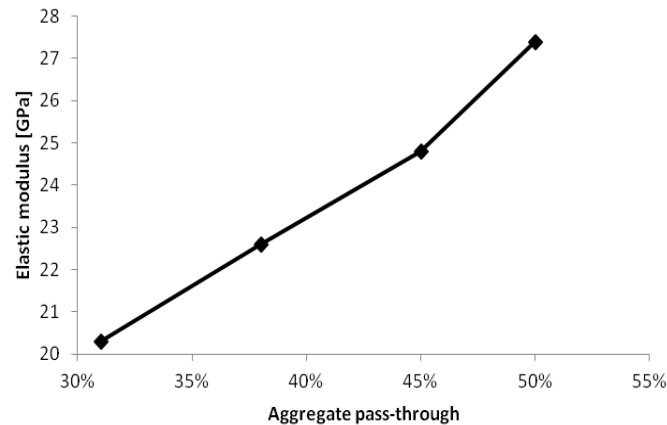
Figure 71: Elastic modulus as a function of aggregate percentage strain gauges passes through

Calculations for elastic modulus of concrete

In this section the models presented in section 2.2.2 will be used to calculated the elastic modulus of a concrete composite. The models are calculated using a constant value for the mortar and having different values for the elastic modulus of the aggregate. The volume of the aggregate is set as 66% and therefore the mortar volume is 34%, where the air content of the concrete is assumed to be part of the mortar. The mortar is given two different values of elastic modulus, i.e. 8 GPa and 15 GPa, which can be considered as a low value and high value respectively. The results of the model calculation are presented in Figure 72 where the elastic modulus of the mortar is 8 GPa and in Figure 73 the results for elastic modulus of 15 GPa. The parallel model overestimates the elastic modulus and the serial model underestimates it. The other three models are to be more representative of the measured modulus of elasticity as the modulus of elasticity should lie somewhere between the parallel model and the serial model. Using the elastic modulus measured in the rock core specimen from quarries 1 and 2 in this chapter and measured values when using the aggregate in concrete, two values were obtained. Theses measured values are shown in Figures 72 and 73, the higher modulus of elasticity is for aggregate from quarry 1 and the lower one is for quarry 2. From the figures it can be seen that the models work when the elastic modulus of the mortar is 8 GPa, but 15 GPa is too high. This is in no way conclusive as there are only two values which are for comparison. From Figure 73 it can be observed that as the modulus of elasticity of the aggregate becomes lower the elastic modulus of the concrete drops quickly both for the model and for the measured values. The

conclusion could be taken that the model by Hirsch and the model by Counto (the models are defined in chapter 2.2.2) work for at least the aggregate from quarry 1, but as the elastic modulus of the mortar is an unknown nothing can be confirmed.

Figure 72: Elastic modulus of the concrete as a function of the elastic modulus of the aggregate for five models and measured values. The models are calculated using 15 GPa for the elastic modulus of mortar
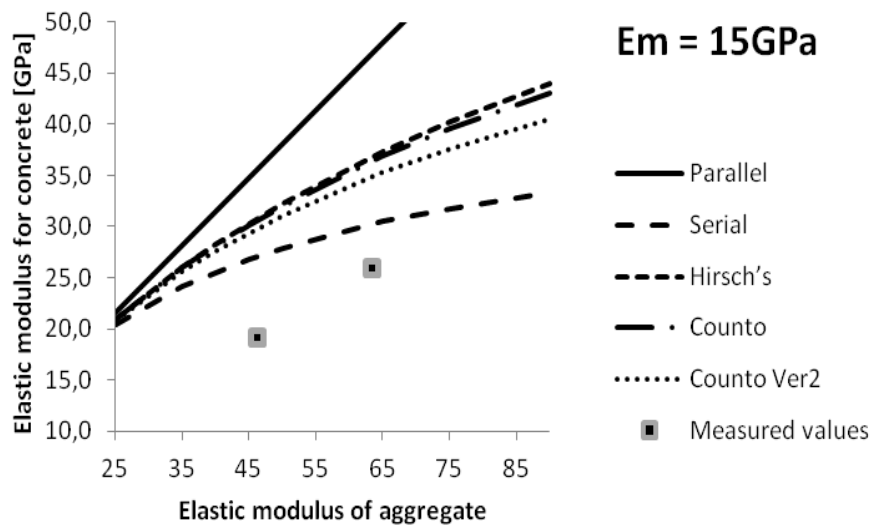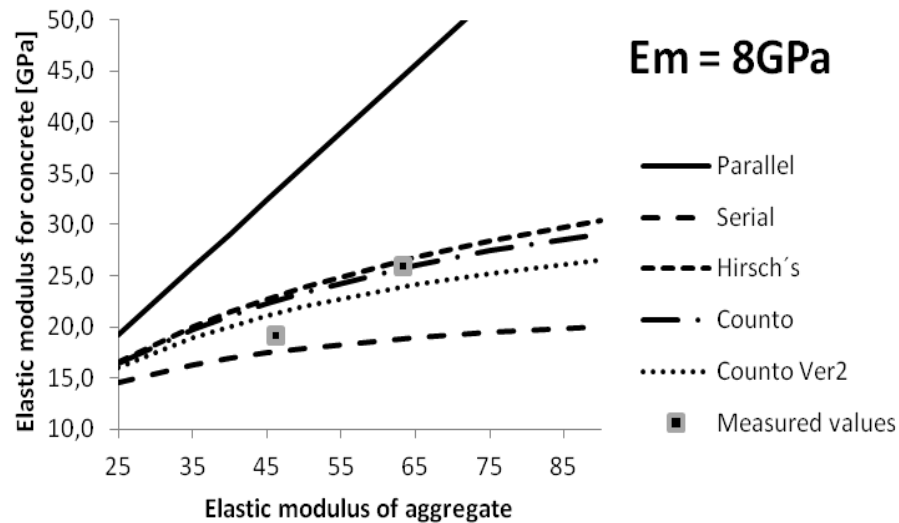

Figure 73: Elastic modulus of the concrete as a function of the elastic modulus of the aggregate for five models and measured values. The models are calculated using 8 GPa for the elastic modulus of mortar

5. Discussions and conclusions

In the first phase of this thesis a study was presented on the long-term research on creep and shrinkage of concrete, which has been carried out at the Innovation Center Iceland for the last decade. This research was presented and analyzed for all the creep rigs that are in use. The results give a good idea on how different type of aggregate (with high to low porosity) and different volume of cement paste affect the concrete composite. Also there results were presented in research on SCC using different amount of cement content and difference in cement paste volume.

From the data in phase 1 it is clear that the porosity of the aggregate influences the creep behavior of the concrete composite. This was observed in nearly all cases. It is known that the elastic modulus of the aggregate is lowered as the porosity increases. The modulus of elasticity is lower for all samples using porous basalt aggregate which is likely to be due to the lower modulus of elasticity of the aggregate. The test on differences in cement paste volume shows that it is clear that with increased volume the creep increases as well, this is considered normal behavior as it is described in ASTM C512.

It has been observed that the creep coefficient and specific creep of SCC are slightly higher (about 10%) than that of SCC with the same binder composition [60]. The result for specific creep in this thesis does not agree with this statement completely, but the samples used for comparison are cast using different types of cement, which affect the shrinkage. It is crucial to observe that the mix-design of SCC made with the Icelandic aggregate and the normal strength concrete are very similar which affect the results. This explains the similarities in the development of the specific creep between mixtures. These two sample types also have similar elastic modulus, which in fact is one of the controlling factors in creep development [36].

In phase 1 there was a comparison of measured creep and predicted values calculated using commonly used models. The models do not agree with measured values and there is a considerably large difference. The largest difference is for concrete made using aggregate from quarry 1 and quarry 3 which do not have the highest porosity. It should be noted that in the calculations for the prediction the measured elastic modulus of the concrete was used. This affects the final creep strain. The porosity of the aggregate affects the stiffness of the concrete due to the lower value for the elastic modulus of the aggregate itself. Therefore, indirectly the porosity of the aggregate affects the final creep strain of the concrete.

In the first phase, shrinkage data was presented and shown that the porosity of the aggregate affects the concrete shrinkage to some extent. The aggregate are a large part of concrete composite, about 60%-75%, and it would be strange if it would not influence the behavior. The research presenting how the increase in porosity increases the volumetric change of the concrete samples and in some cases the increase was about 33% where the increase in porosity was about 50% higher. This could be because of the increased volume of water in the sample which could affect the amount of water that vaporized during the drying out of the sample. Where there is more volume of water and more of it vaporizes the volumetric changes of the concrete sample increases.

Estimated values for shrinkage using commonly used models were presented and evaluated against the collected measured data. It showed that EC2 underestimates the final shrinkage of concrete samples. ACI209 overestimated the shrinkage in nearly all cases. This difference could be due to the fact that the model in EC2 does not take enough factors into account, where ACI209 takes many factors but overestimates the values. Both of these models do not take into consideration the porosity of the aggregate and in some cases it should be considered to take this factor into account as it obviously affects the behavior.

In the second phase of this thesis there was a study of the porosity of aggregate and its effects on the mechanical properties of the concrete composite. This was of interest, as it has been observed in the past that as the aggregate become more porous the elastic modulus of the concrete lowers. To test this, samples from two of the quarries (same as in phase 1) were chosen to test the porosity versus the mechanical properties of the rock material (the aggregate). This was done as well as the test of the porosity using x-ray tomography. The acquired results were then compared using models for estimating elastic modulus of concrete.

The intact core specimen were tested for porosity, this was done with two methods for comparison. The first method is a commonly used method for large aggregate, where the water absorption and density are measured. The first method to evaluate the porosity of the aggregate was derived from the density and water absorption. The second method is the x-ray tomography, where the total volume and void volume are measured from the 3D scan. The porosities of these two methods seem to show similar values when the porosity is low (around 3%), but as the porosity increases there is a divergence of the method, the x-ray method appears to show higher porosity. This is due to the fact that the common method (aggregate testing method for density and water absorption) uses water to measure the porosity. The method assumes that water can penetrate the voids in the system but this is incorrect. The x-ray tomography can scan the total material and is more accurate and measure more voids.

The mechanical properties of the intact core specimen were tested to compare them to the porosity and density of the aggregate. This was to see the connection between the elements of the materials and evaluate their effect on the properties of concrete when used in concrete mixtures. There was a definite relation between the porosity of the material and the elastic modulus; with increased porosity there was a significant decrease in elastic modulus. A further research is needed to indicate how the porosity relates to elastic modulus and to be able to predict it. The ultimate compressive strength was also tested and indicated a decrease in strength with lower porosity but it was inconclusive. This indicates that the porosity of the aggregate has negative effects on the mechanical properties of the aggregate and therefore the concrete composite. The density of the aggregate was also compared to the elastic modulus and found to have an inconclusively linear relation. This behavior of material is well known so this in fact gives the results added value. The connection of the ultimate compressive strength to the density was not as good as for the elastic modulus, but has good linear connection; as the density increases the strength increases.

There were cast a number of specimen from two concrete mixture to get an idea on how efficient the measurement methods are. The results were good for the cylinders 150x300mm, they gave good correlation between specimen. For the drilled concrete cores the results were significantly more scattered. There was also a large difference between values measured with strain gauges and compressometer. This was shown to be caused by the localized effects of the aggregate on the strain gauges. As the strain gauges measure less strain if it is in touch with more aggregate and due to this fact the evaluated elastic modulus becomes greater.

Some concrete models for estimating the elastic modulus of the concrete were evaluated. These models take the two main phases of the concrete (mortar and aggregate) and calculate the elastic modulus of the concrete composite. There are the two main models, parallel model and serial model which give an overestimated elastic modulus and an underestimated one, representatively. The conclusion of the study was that the three other models (which actually are all combination of parallel model and serial model) give a good quality evaluation for the combination of the elastic modulus. The models were only compared to two measured values where the elastic modulus of the mortar was an unknown. This gave no valid conclusion whether the models work but it was evident that more research on this is needed.

There are obvious connections between the increased porosity of the aggregate and the increased creep and shrinkage. This is known because of the connection of the elastic modulus to the volumetric stability of the concrete and the conclusive evidence of the connection of the porosity of the aggregates to the elastic modulus of concrete. This gives the conclusion that the porosity of the aggregate in fact increases the creep and shrinkage of the concrete composite.

Conclusions

• Higher creep strain is observed in concrete made with aggregate of higher porosity.

• Specific creep of the samples suggests that the development of creep is influenced by the type of aggregate. As aggregate become more porous the less effect the strength class of the concrete has on the creep. This could be due to the fact that when aggregate get less stiff (due to higher porosity) there is more load applied to the cement paste, which reduces the scatter of results between different strength classes when using porous aggregate.

• All the creep models fail in prediction the development of creep over long time regardless of the concrete type, although some models predict the final creep strain approximately correctly.

• The models from the EC2 design code and ACI209 underestimate creep in most cases, except for specimen made with very porous aggregate.

• The B3 model overestimates creep for the porous basalt aggregate, regardless of the concrete type.

• A drastic reduction is observed in the modulus of elasticity of the concrete when using porous aggregate. An increase in porosity of 15% can lower the elastic modulus of the concrete by up to 40%.

• It has been shown that the porosity of the aggregate has considerable effects on the shrinkage behavior.

•   It has been shown that there is a link between the porosity of the aggregate and shrinkage, but more research is needed to understand this behavior and predict it.

•   The elastic modulus of the aggregate is inconclusively in connection to the porosity of the material, with increased porosity gives lower elastic modulus.

•   The x-ray tomography analyzes gives higher values in porosity than the commonly known aggregate testing method.

•   There is a good relation of the density of the aggregate to the elastic modulus of the aggregate.

•   The models for concrete composite give good evaluation using the elastic modulus of the aggregate and mortar.

•   Strain gauge measurement of concrete drilled cores gives higher values for elastic modulus due to localized effects of the aggregate.

•   Concrete composite is obviously affected by increased porosity of aggregate; if the porosity is high the elastic properties of the aggregate are low and therefore the concretes.

6. References

[1]   Z. Bažant, "Prediction of concrete creep and shrinkage: past, present and future," *Nuclear Engineering and Design*, vol. 203, pp. 27–38, 2001.

[2]   T. Megson, *Structural and stress analysis*. Butterworth-Heinemann, 1996.

[3]   M. Collepardi, *The new concrete*. Grafiche Tintoretto, 2006.

[4]   H. Lechtman, L. Hobbs, and W. Kingery, "Roman concrete and the roman architectural revolution," *Country: United States*, vol. 3, pp. 81–128, 1986.

[5]   L. C. Lancaster, *Concrete Vaulted Construction in Imperial Rome: Innovations in Context*. Cambridge University Press, 2005.

[6]   H. J. Cowan, *The Master-builders*. John Wiley & Sons Inc, 1978.

[7]   E. Higginson, "Mineral admixtures," *Significance of Tests and Properties of Concrete and Concrete-Making Materials*, pp. 543–555, 1966.

[8]   P. Mehta, "Mineral admixtures," *VS Ramachandran, Noyes Publication, Park Ridge, New Jersey, USA*, pp. 303–333, 1984.

[9]   J. Damtoft, J. Lukasik, D. Herfort, D. Sorrentino, and E. Gartner, "Sustainable development and climate change initiatives," *Cement and concrete research*, vol. 38, no. 2, pp. 115–127, 2008.

[10]   O. Wallevik, "The rheology of fresh concrete and its application on concrete with and without silica fume," Ph.D. dissertation, Trondheim, 1990.

[11]   O. Wallevik and J. Wallevik, "Rheology as a tool in concrete science: The use of rheographs and workability boxes," *Cement and Concrete Research*, 2011.

[12]   R. Bakker, "Permeability of blended cement concretes," in *Proceedings of the*, 1983.

[13]   T. Zohdi, P. Monteiro, and V. Lamour, "Extraction of elastic moduli from granular compacts," *International journal of fracture*, vol. 115, no. 3, pp. 49–54, 2002.

[14]   M. Ayhan, H. Gönül, I. Gönül, and A. Karakus, "Effect of basic pumice on morphologic properties of interfacial transition zone in load-bearing lightweight/semi-lightweight concretes," *Çonstruction and Building Materials*, vol. 25, no. 5, pp. 2507–2518, 2011.

[15]   U. Counto, "The effect of the elastic modulus of the aggregate on the elastic modulus, creep and creep recovery of concrete," *Magazine of Concrete Research*, vol. 16, no. 48, pp. 129–138, 1964.

[16]   J. H. S. Þorgeir S. Helgason, "Rock types and technical properties of rock materials (in icelandic)," Icelandic Building research institute, Tech. Rep., 1996.

[17]   F. Nabarro, "Do we have an acceptable model of power-law creep?" *Materials Science and Engineering A*, vol. 387, pp. 659–664, 2004.

[18]   F. Nabarro and H. De Villiers, *The physics of creep: Creep and creep-resistant alloys*. CRC, 1995.

[19]   B. Engström, *Restraint cracking of reinforced concrete structures*, 2006.

[20]   A. Neville and J. Brooks, *Concrete Technology*. Prentice-Hall, 2010.

[21]   G. Pickett, "The effect of change in moisture content on the creep of concrete under a sustained load," *ACI Journal*, no. 15, pp. 333–356, 1942.

[22]   Z. Bažant and E. Osman, "Double power law for basic creep of concrete," *Materials and Structures*, vol. 9, no. 1, pp. 3–11, 1976.

[23]   G. Jónsson, *Deformation of Concrete - Elastic modulus and creep - (In Icelandic).* Icelandic Building research institute, 2006.

[24]   F. Wittmann and P. Roelfstra, "Total deformation of loaded drying concrete," *Cement and Concrete Research*, vol. 10, no. 5, pp. 601–610, 1980.

[25]   F. Wittmann, "On the influence of stress on shrinkage of concrete," in *RILEM PROCEEDINGS*. CHAPMAN & HALL, 1993, pp. 151–151.

[26]   Z. Bažant and J. Chern, "Concrete creep at variable humidity: constitutive law and mechanism," *Materials and structures*, vol. 18, no. 18, pp. 1–20, 1985.

[27]   Z. Bažant and X. Yunping, "Drying creep of concrete: constitutive model and new experiments separating its mechanisms," *Materials and Structures*, vol. 27, no. 1, pp. 3–14, 1994.

[28]   Z. Bažant and L. Robert, *Mathematical modeling of creep and shrinkage of concrete*. Wiley, 1988.

[29]   S. Altoubat and D. Lange, "The pickett effect at early age and experiment separating its mechanisms in tension," *Materials and Structures*, vol. 35, no. 4, pp. 211–218, 2002.

[30]   J. Brooks, "30-year creep and shrinkage of concrete," *Magazine of concrete research*, vol. 57, no. 9, pp. 545–556, 2005.

[31]   M. Ortiz, "A constitutive theory for the inelastic behavior of concrete," *Mechanics of Materials*, vol. 4, no. 1, pp. 67–93, 1985.

[32]   M. Ortiz and E. Popov, "A physical model for the inelasticity of concrete," *Proceedings of the Royal Society of London. A. Mathematical and Physical Sciences*, vol. 383, no. 1784, pp. 101–125, 1982.

[33]   J. Shao, Q. Zhu, and K. Su, "Modeling of creep in rock materials in terms of material degradation," *Computers and Geotechnics*, vol. 30, no. 7, pp. 549–555, 2003.

[34]   J. Wastiels, "Behaviour of concrete under multiaxial stresses—a review," *Cement and Concrete Research*, vol. 9, no. 1, pp. 35–44, 1979.

[35]   D. Drucker, W. Prager, and H. Greenberg, "Extended limit design theorems for continuous media," *Quarterly of Applied Mathematics*, vol. 9, no. 4, pp. 381–389, 1952.

[36]   Z. Bažant and S. Prasannan, "Solidification theory for concrete creep. i: Formulation," *Journal of Engineering Mechanics*, vol. 115, no. 8, pp. 1691–1703, 1989.

[37]   Z. Bažant, "Viscoelasticity of porous solidifying material—concrete," *J. Eng. Mech. Div*, vol. 103, pp. 1049–10067, 1977.

[38]   Z. Bažant and S. Kim, "Nonlinear creep of concrete—adaptation and flow," *Journal of the Engineering Mechanics Division*, vol. 105, no. 3, pp. 429–446, 1979.

[39]   Z. Bažant, "Theory of creep and shrinkage in concrete structures: A precis of recent developments," *Mechanics today*, vol. 2, pp. 1–93, 1975.

[40]   H. Jennings, "Colloid model of c- s- h and implications to the problem of creep and shrinkage," *Materials and structures*, vol. 37, no. 30, pp. 59–70, 2004.

[41]   P. Tennis and H. Jennings, "A model for two types of calcium silicate hydrate in the microstructure of portland cement pastes," *Cement and Concrete Research*, vol. 30, no. 6, pp. 855–863, 2000.

[42]   J. Thomas and H. Jennings, "A colloidal interpretation of chemical aging of the csh gel and its effects on the properties of cement paste," *Cement and concrete research*, vol. 36, no. 1, pp. 30–38, 2006.

[43]   C. Lynam, *Growth and movement in Portland cement concrete*. Oxford University Press, 1934.

[44]   Y. Lee, S. Yi, M. Kim, and J. Kim, "Evaluation of a basic creep model with respect to autogenous shrinkage," *Cement and concrete research*, vol. 36, no. 7, pp. 1268–1278, 2006.

[45]   B. M. Das, *Principles of Geotechnical Engineering*. Thomson-Engineering, 2001.

[46]   A. M. Neville, *Properties of Concrete: Fourth and Final Edition*. Wiley, 1996.

[47]   E. Maranini and M. Brignoli, "Creep behaviour of a weak rock: experimental characterization," *International Journal of Rock Mechanics and Mining Sciences*, vol. 36, no. 1, pp. 127–138, 1999.

[48]   Y. Fujii, T. Kiyama, Y. Ishijima, and J. Kodama, "Circumferential strain behavior during creep tests of brittle rocks," *International Journal of Rock Mechanics and Mining Sciences*, vol. 36, no. 3, pp. 323–337, 1999.

[49]   F. Bourgeois, J. Shao, and O. Ozanam, "An elastoplastic model for unsaturated rocks and concrete," *Mechanics Research Communications*, vol. 29, no. 5, pp. 383–390, 2002.

[50]   D. Singh, "A study of creep of rocks," in *International Journal of Rock Mechanics and Mining Sciences & Geomechanics Abstracts*, vol. 12, no. 9. Elsevier, 1975, pp. 271–276.

[51]   M. G. Alexander and S. Mindess, *Aggregates in Concrete (Modern Concrete Technology)*. Spon Press, 2005.

[52]   C. Eurocode, *Eurocode 2: Design of concrete structures–Part 1-1: General rules and rules for buildings*, 2003.

[53]   ACI209.R2, *Prediction of Creep, Shrinkage, and Temperature Effects in Concrete Structures*. ACI Committee 209, 1997.

[54]   Z. Bažant and S. Baweja, "Creep and shrinkage prediction model for analysis and design of concrete structures: Model b3," *ACI SPECIAL PUBLICATIONS*, vol. 194, pp. 1–84, 2000.

[55]   C. ASTM, "512,"," *Test Method for Creep of Concrete in Compression," American Society of Testing and Materials, West Conshohocken, Penn*.

[56]   ASTM-C157, "Standard test method for length change of hardened hydraulic-cement mortar and concrete," Tech. Rep., 1999.

[57]   B. EN, "1097-6: 2000," *Tests for mechanical and physical properties of aggregates-Part 6: determination of particle density and water absorption*.

[58]   D. ASTM, "7012,"," *Standard Test Method for Compressive Strength and Elastic Moduli of Intact Rock Core Specimens under Varying States of Stress and Temperatures,"* American Society of Testing and Materials, West Conshohocken, Penn*.

[59]   ASTM-C469, "Standard test method for static modulus of elasticity and poisson's ratio of concrete in compression," Tech. Rep., 1994.

[60]   M. Vieira, A. Bettencourt, O. Wallevik, and I. Nielsson, "Deformability of hardened scc," *year: 2003*, pp. 637–644, 2003.